Monte Carlo evaluation of path integrals for the nuclear shell model

G. H. Lang, C. W. Johnson,* S. E. Koonin, and W. E. Ormand

*W. K. Kellogg Radiation Laboratory, 106-38, California Institute of Technology,
Pasadena, California 91125*

(Received 12 May 1993)

We present in detail a formulation of the shell model as a path integral and Monte Carlo techniques for its evaluation. The formulation, which linearizes the two-body interaction by an auxiliary field, is quite general, both in the form of the effective "one-body" Hamiltonian and in the choice of ensemble. In particular, we derive formulas for the use of general (beyond monopole) pairing operators, as well as a novel extraction of the canonical (fixed-particle-number) ensemble via an activity expansion. We discuss the advantages and disadvantages of the various formulations and ensembles and give several illustrative examples. We also discuss and illustrate calculation of the imaginary-time response function and the extraction, by maximum entropy methods, of the corresponding strength function. Finally, we discuss the "sign problem" generic to fermion Monte Carlo calculations, and prove that a wide class of interactions are free of this limitation.

PACS number(s): 21.60.Cs, 21.60.Ka, 02.70.−c

I. MOTIVATION AND ORGANIZATION

Exact diagonalizations of shell model Hamiltonians in the $0s$-$1d$ shell demonstrated [1] that the shell model can yield an accurate and consistent description for a wide range of nuclear properties in different nuclei, if the many-body basis is sufficiently large. However, the combinatorial scaling of the many-body space with the size of the single-particle basis or the number of valence nucleons restricts such exact diagonalizations to small nuclei or nuclei with few valence particles [2].

In facing the general challenge of developing nonperturbative methods to describe strongly interacting many-body systems, various quantum Monte Carlo schemes have been proposed as an alternative to direct diagonalization [3]. Among them, the auxiliary-field Monte Carlo method is suitable for addressing interacting fermions [4]. This method is a Monte Carlo evaluation of the path integral obtained by the Hubbard-Stratonovich transformation [5] of the imaginary-time evolution operator. The many-body wave function is represented by a set of determinantal wave functions evolving in fluctuating auxiliary fields. The method thus enforces the Pauli principle exactly, and the storage and computation time scale gently with the single-particle basis or the number of particles. Auxiliary-field methods have been applied to condensed matter systems such as the Hubbard model [3,6], yielding important information about electron correlations and magnetic properties.

In this paper, we discuss the application of auxiliary-field Monte Carlo techniques to the nuclear shell model.

This involves a two-body interaction more general than the simple on-site repulsion of a Hubbard model. Our goal is to develop new methods for extending the applicability of the shell model, as well as to investigate the powers and limitations of auxiliary-field Monte Carlo methods for general fermion systems.

We have previously published a Letter [7] with selected results for static observables in sd- and fp-shell nuclei. This paper serves to give the details of the implementation, introduce a method for calculating dynamical correlations and strength functions, demonstrate the method with simple (sd-shell) nuclei, and discuss several important issues that arise in the implementation. We also explore the limitations imposed by the negative contributions in the path integral, referred to as the "sign problem" in the literature.

Our presentation is organized as follows. We begin in Sec. II by using the Hubbard-Stratonovich (HS) transformation to write the imaginary-time evolution operator $\exp(-\beta\hat{H})$ as a path integral. This requires that the Hamiltonian $\hat{H}$ be cast as a quadratic form using an appropriate set of operators. We discuss in Sec. III two ways in which this can be accomplished, using either particle density or pairing operators. The imaginary-time evolution operator can be used to extract information about the system at finite temperature or in its ground state ($\beta \to \infty$). The formulas for obtaining static observables are presented in Sec. IV where methods for handling the canonical ensemble are also introduced. We then discuss in Sec. V the extraction of the strength functions for operators from the imaginary-time response function. In Sec. VI, we briefly describe the computational algorithms for implementing our methods and present selected results of calculations for sd-shell nuclei. In the final section, we address the sign problem and also discuss a class of nontrivial interactions that give rise to a positive definite path integral for some nuclei.

---

*Present address: Los Alamos National Laboratory, T-5, Mail Stop B283, P. O. Box 1663, Los Alamos, NM 87545.

II. IMAGINARY-TIME EVOLUTION OPERATOR

Given some many-body Hamiltonian $\hat{H}$, we seek a tractable expression for the imaginary-time evolution operator:

$$\hat{U} = \exp(-\beta\hat{H}) . \tag{2.1}$$

Here, β has units of inverse energy and β^{-1} can be interpreted as an imaginary time. (Here and throughout, we take $\hbar = 1$ and measure all energies in units of MeV.) It is also clear that $\hat{U}$ can be interpreted as the partition operator for temperature β^{-1}. We will refer to $\hat{U}$ as the evolution operator hereafter. The operator $\hat{H}$ is usually a generalized Hamiltonian and might contain terms beyond the true Hamiltonian, such as $-\mu\hat{N}$ in the grand-canonical ensemble or $-\omega\hat{J}_z$ if we are "cranking" the system.

There are two formalisms for extracting information from the evolution operator: the "thermal" formalism (on which we will concentrate) and the "zero-temperature" formalism (to which the thermal formalism reduces in the limit $\beta \rightarrow \infty$). In the thermal formalism, we begin with the partition function

$$Z = \hat{\mathrm{Tr}}\exp(-\beta\hat{H}) , \tag{2.2}$$

and then construct the thermal observable of an operator $\hat{O}$:

$$\langle\hat{O}\rangle = \frac{1}{Z}\hat{\mathrm{Tr}}\left[\hat{O}\exp(-\beta\hat{H})\right] . \tag{2.3}$$

Here, the trace $\hat{\mathrm{Tr}}$ is over many-body states of fixed (canonical) or all (grand-canonical) particle number. In the zero-temperature formalism we begin with a trial wave function ψ_0 and use the evolution operator to project out the ground state, assuming that ψ_0 is not orthogonal to the ground state. The expectation value of $\hat{O}$ is then given by

$$\langle\hat{O}\rangle = \lim_{\beta\rightarrow\infty}\frac{\langle\psi_0|\exp(-\frac{\beta}{2}\hat{H})\hat{O}\exp(-\frac{\beta}{2}\hat{H})|\psi_0\rangle}{\langle\psi_0|\exp(-\beta\hat{H})|\psi_0\rangle} . \tag{2.4}$$

In this section, we describe how to write $\hat{U}$ in a form that allows Eq. (2.3) or (2.4) to be evaluated.

A. Path-integral formulation of the evolution operator

We restrict ourselves to generalized Hamiltonians that contain at most two-body terms. The Hamiltonian $\hat{H}$ can then be written as a quadratic form in some set of "convenient" operators $\hat{\mathcal{O}}_\alpha$:

$$\hat{H} = \sum_\alpha \epsilon_\alpha \hat{\mathcal{O}}_\alpha + \frac{1}{2}\sum_\alpha V_\alpha \hat{\mathcal{O}}_\alpha^2 , \tag{2.5}$$

where we have assumed that the quadratic term is diagonal in the $\hat{\mathcal{O}}_\alpha$. The meaning of "convenient" will become clear shortly, but typically it refers to one-"body" operators, either one particle ("density") or one quasiparticle ("pairing"). The strength of the two-body interaction is characterized by the real numbers V_α.

For $\hat{H}$ in the quadratic form (2.5), one can write the evolution operator $\hat{U}$ as a path integral. The exponential is first split into N_t "time" slices, $\beta = N_t\Delta\beta$, so that

$$\hat{U} = \left[\exp(-\Delta\beta\hat{H})\right]^{N_t} . \tag{2.6}$$

Then we perform the Hubbard-Stratonovich (HS) transformation on the two-body term for the nth time slice to give [5]

$$\exp\left(-\Delta\beta\hat{H}\right) \simeq \int_{-\infty}^{\infty}\prod_\alpha d\sigma_{\alpha n}\left(\frac{\Delta\beta|V_\alpha|}{2\pi}\right)^{1/2}\exp\left\{-\Delta\beta\left(\sum_\alpha\frac{1}{2}|V_\alpha|\sigma_{\alpha n}^2 + \epsilon_\alpha\hat{\mathcal{O}}_\alpha + s_\alpha V_\alpha\sigma_{\alpha n}\hat{\mathcal{O}}_\alpha\right)\right\} , \tag{2.7}$$

where the phase factor s_α is ± 1 if $V_\alpha < 0$ and is $\pm i$ if $V_\alpha > 0$. Each real variable $\sigma_{\alpha n}$ is the *auxiliary field* associated with $\hat{\mathcal{O}}_\alpha$ at time slice n.

The approximation (2.7) is valid through order $\Delta\beta$, since the corrections are commutator terms of order $(\Delta\beta)^2$. The evolution operator is then

$$\hat{U} = \left[\exp\left(-\Delta\beta\hat{H}\right)\right]^{N_t} \simeq \int \mathcal{D}^{N_t}[\sigma]G(\sigma)\exp\left[-\Delta\beta h_\sigma\left(\tau_{N_t}\right)\right]\cdots\exp\left[-\Delta\beta h_\sigma\left(\tau_1\right)\right] , \tag{2.8}$$

where the integration measure is

$$\mathcal{D}^{N_t}[\sigma] = \prod_{n=1}^{N_t}\prod_\alpha d\sigma_{\alpha n}\left(\frac{\Delta\beta|V_\alpha|}{2\pi}\right)^{\frac{1}{2}} , \tag{2.9a}$$

the Gaussian factor is

$$G(\sigma) = \exp\left(-\sum_{\alpha n}\frac{1}{2}|V_\alpha|\sigma_{\alpha n}^2\right) , \tag{2.9b}$$

and the one-body Hamiltonian is

$$\hat{h}_\sigma(\tau_n) = \sum_\alpha \left(\epsilon_\alpha + s_\alpha V_\alpha\sigma_{\alpha n}\right)\hat{\mathcal{O}}_\alpha . \tag{2.10}$$

It is sometimes convenient to employ a continuum notation

$$\hat{U} = \int \mathcal{D}\,[\sigma] \exp\left(-\frac{1}{2}\int_0^\beta d\tau \sum_\alpha |V_\alpha|\,\sigma_\alpha^2(\tau)\right)$$

$$\times \left[\mathcal{T}\exp\left(-\int_0^\beta d\tau\,\hat{h}_\sigma(\tau)\right)\right] ,\qquad (2.11)$$

where $\mathcal{T}$ denotes time ordering and

$$\mathcal{D}\,[\sigma] = \lim_{N_t\to\infty} \mathcal{D}^{N_t}[\sigma] ,\qquad (2.12)$$

$$\mathcal{T}\exp\left(-\int_0^\beta d\tau\,\hat{h}_\sigma(\tau)\right) = \lim_{N_t\to\infty}\prod_{n=1}^{N_t}\exp\left[-\Delta\beta\,\hat{h}_\sigma(\tau_n)\right] .$$

$$(2.13)$$

In the limit of an infinite number of time slices Eq. (2.8) is exact. In practice one has a finite number of time slices and the approximation is valid only to order $\Delta\beta$. The case of only one time slice is known as the static path approximation (SPA); previous work on the SPA and its extensions can be found in Refs. [8] and [9].

Rewriting the evolution operator as a path integral can make the model space tractable. Consider the case where the $\hat{\mathcal{O}}_\alpha$ are density operators. Then Eq. (2.1) is an exponential of two-body operators; it acts on a Slater determinant to produce a sum of many Slater determinants. In contrast, the path-integral formulation (2.8) contains only exponentials of one-body operators which, by Thouless's theorem [10], takes a Slater determinant to another single Slater determinant. Therefore, instead of having to keep track of a very large number of determinants (often many thousands for modern matrix-diagonalization shell model codes such as OXBASH [11]), we need deal only with one Slater determinant at a time. Of course, the price to be paid is the evaluation of a high-dimensional integral. However, the number of auxiliary fields grows only quadratically with the size of the single-particle basis while the corresponding number of Slater determinants grows exponentially. Furthermore, the integral can be evaluated stochastically, making the problem ideal for parallel computation.

B. Monte Carlo evaluation of the path integral

Formulating the evolution operator as a path integral over auxiliary fields reduces the problem to quadrature. For a limited number of auxiliary fields, such as in the SPA with only a quadrupole-quadrupole interaction, the integral can be evaluated by direct numerical quadrature. However, for more general cases (typically hundreds of fields), the integral must be evaluated stochastically using Monte Carlo techniques.

Using the one-body evolution operator defined by

$$\hat{U}_\sigma(\tau_2,\tau_1) = \mathcal{T}\exp\left(-\int_{\tau_1}^{\tau_2} d\tau\,\hat{h}_\sigma(\tau)\right) ,\qquad (2.14)$$

we can write Eq. (2.3) or (2.4) as

$$\langle\hat{O}\rangle = \frac{\int \mathcal{D}\,[\sigma]\,G(\sigma)\langle\hat{O}(\sigma)\rangle\zeta(\sigma)}{\int \mathcal{D}\,[\sigma]\,G(\sigma)\,\zeta(\sigma)} .\qquad (2.15)$$

For the zero-temperature formalism

$$\zeta(\sigma) \equiv \langle\psi_0|\hat{U}_\sigma(\beta,0)|\psi_0\rangle \qquad (2.16)$$

and

$$\langle\hat{O}(\sigma)\rangle = \frac{\langle\psi_0|\hat{U}_\sigma(\beta,\beta/2)\,\hat{O}\,\hat{U}_\sigma(\beta/2,0)|\psi_0\rangle}{\langle\psi_0\left|\hat{U}_\sigma(\beta,0)\right|\psi_0\rangle} ,\qquad (2.17)$$

while for the thermal formalism (canonical and grand canonical),

$$\zeta(\sigma) \equiv \hat{\mathrm{Tr}}[\hat{U}_\sigma(\beta,0)] \qquad (2.18)$$

and

$$\langle\hat{O}\rangle_\sigma = \frac{\hat{\mathrm{Tr}}\left[\hat{O}\,\hat{U}_\sigma(\beta,0)\right]}{\hat{\mathrm{Tr}}\hat{U}_\sigma(\beta,0)} .\qquad (2.19)$$

To evaluate the path integral via Monte Carlo techniques, we must choose a normalizable positive-definite weight function W_σ, and generate an ensemble of statistically independent fields $\{\sigma_i\}$ such that the probability density to find a field with values σ_i is W_{σ_i}. Defining the "action" by

$$\mathcal{S}_\sigma = \sum_\alpha \frac{1}{2}|V_\alpha|\int_0^\beta d\tau\,\sigma_\alpha(\tau)^2 - \ln\zeta(\sigma) ,\qquad (2.20)$$

the required observable is then simply

$$\langle\hat{O}\rangle = \frac{\int \mathcal{D}\,[\sigma]\,\langle\hat{O}\rangle_\sigma e^{-\mathcal{S}_\sigma}}{\int \mathcal{D}\,[\sigma]\,e^{-\mathcal{S}_\sigma}} = \frac{\frac{1}{N}\sum_i\langle\hat{O}\rangle_i\Phi_i}{\frac{1}{N}\sum_i\Phi_i} ,\qquad (2.21)$$

where N is the number of samples,

$$\Phi_i = e^{-\mathcal{S}_i}/W_i \qquad (2.22)$$

and $\mathcal{S}_i \equiv \mathcal{S}_{\sigma_i}$, etc. Ideally W should approximate $\exp(-\mathcal{S})$ closely. However, $\exp(-\mathcal{S})$ is generally not positive and can even be complex. In some cases, Φ_i may oscillate violently, giving rise to a very small denominator in Eq. (2.21) to be canceled by a very small numerator. While this cancellation is exact analytically, it is only approximate in the Monte Carlo evaluation so that this "sign problem" leads to large variances in the evaluation of the observable.

There are several possible schemes for both the choice of W and the sampling of the fields. We typically choose $W = |\exp(-\mathcal{S})|$ and generate the samples via random walk (Metropolis) methods.

III. DECOMPOSITIONS OF THE HAMILTONIAN

To realize the HS transformation, the two-body parts of $\hat{H}$ must be cast as a quadratic form in one-body operators $\hat{\mathcal{O}}_\alpha$. As these latter can be either density opera-

tors or pair creation and annihilation operators (or both), there is considerable freedom in doing so. In the simplest example, let us consider an individual interaction term

$$\hat{H} = a_1^\dagger a_2^\dagger a_4 a_3 ,$$ (3.1)

where $a_i^\dagger, a_i$ are anticommuting fermion creation and annihilation operators. In the pairing decomposition, we write (using the upper and lower brackets to indicate the grouping)

$$\hat{H} = \overbrace{a_1^\dagger a_2^\dagger} \underbrace{a_4 a_3}$$ (3.2a)

$$= \frac{1}{4}(a_1^\dagger a_2^\dagger + a_3 a_4)^2 - \frac{1}{4}(a_1^\dagger a_2^\dagger - a_3 a_4)^2$$

$$+ \frac{1}{2}[a_1^\dagger a_2^\dagger, a_3 a_4] .$$ (3.2b)

The commutator is a one-body operator that can be put directly in the one-body Hamiltonian $\hat{h}_\sigma$. The remaining two quadratic forms in pair creation and annihilation operators can be coupled to auxiliary fields in the HS transformation.

In the density decomposition, there are two ways to proceed: We can group (1, 3) and (2, 4) to get

$$\hat{H} = \overbrace{a_1^\dagger a_3} \underbrace{a_2^\dagger a_4} - a_1^\dagger a_4 \delta_{23}$$ (3.3a)

$$= -a_1^\dagger a_4 \delta_{23} + \frac{1}{2}[a_1^\dagger a_3, a_2^\dagger a_4] + \frac{1}{4}(a_1^\dagger a_3 + a_2^\dagger a_4)^2$$

$$- \frac{1}{4}(a_1^\dagger a_3 - a_2^\dagger a_4)^2 ,$$ (3.3b)

or group (1, 4) and (2, 3) to get

$$\hat{H} = - \overbrace{a_1^\dagger a_4} \underbrace{a_2^\dagger a_3} + a_1^\dagger a_3 \delta_{24} .$$ (3.4a)

$$= a_1^\dagger a_3 \delta_{24} - \frac{1}{2}[a_1^\dagger a_4, a_2^\dagger a_3] - \frac{1}{4}(a_1^\dagger a_4 + a_2^\dagger a_3)^2$$

$$+ \frac{1}{4}(a_1^\dagger a_4 - a_2^\dagger a_3)^2 .$$ (3.4b)

Again the commutator terms are one-body operators, but now the quadratic forms are squares of density operators that conserve particle number. We refer to Eq. (3.3) as the "direct" decomposition and Eq. (3.4) as the "exchange" decomposition.

For any general two-body Hamiltonian, we can choose the pairing or density decompositions for different parts of the two-body interaction. Moreover, even within a pure density breakup decomposition, there is still freedom to choose between the direct and exchange formulations. Although the exact path-integral result is independent of the scheme used, different schemes will lead to different results under certain approximations (e.g., mean field or SPA). The choice of decomposition will also affect the rate of convergence of our numerical result as $N_t \to \infty$, as well as the statistical precision of the Monte Carlo evaluation. Most significantly, it affects the fluctuation of Φ in Eq. (2.21) and thus determines the stability of the Monte Carlo calculation. (See Sec. VI below.)

In the application of these methods to the nuclear shell model, it is particularly convenient to use quadratic forms of operators that respect rotational invariance, isospin symmetry, and the shell structure of the system. We introduce these in the following subsections for both the density and pairing decompositions.

A. Density decomposition

We begin by ignoring explicit isospin labels and by writing the rotationally invariant two-body Hamiltonian as

$$\hat{H}_2 = \frac{1}{2}\sum_{abcd}\sum_J V_J(ab, cd)\sum_M A_{JM}^\dagger(ab)A_{JM}(cd)$$

$$= \frac{1}{4}\sum_{abcd}\sum_J [(1 + \delta_{ab})(1 + \delta_{cd})]^{1/2}\, V_J^A(ab, cd)$$

$$\times \sum_M A_{JM}^\dagger(ab)A_{JM}(cd) ,$$ (3.5)

where the sum is taken over all proton and neutron single-particle orbits (denoted by a, b, c, d) and the pair creation and annihilation operators are given by

$$A_{JM}^\dagger(ab) = \sum_{m_a m_b}(j_a m_a j_b m_b|JM)a_{j_b m_b}^\dagger a_{j_a m_a}^\dagger$$

$$= -[a_{j_a}^\dagger \times a_{j_b}^\dagger]^{JM} ,$$ (3.6a)

$$A_{JM}(ab) = \sum_{m_a m_b}(j_a m_a j_b m_b|JM)a_{j_a m_a} a_{j_b m_b}$$

$$= [a_{j_a} \times a_{j_b}]^{JM} .$$ (3.6b)

The $V_J(ab, cd)$ are the angular momentum coupled two-body matrix elements of a scalar potential $V(\mathbf{r}_1, \mathbf{r}_2)$ defined as

$$V_J(ab, cd) = \langle [\psi_{j_a}(\mathbf{r}_1) \times \psi_{j_b}(\mathbf{r}_2)]^{JM}$$

$$\times |V(\mathbf{r}_1, \mathbf{r}_2)| [\psi_{j_c}(\mathbf{r}_1) \times \psi_{j_d}(\mathbf{r}_2)]^{JM} \rangle$$ (3.7)

(independent of M) while the antisymmetrized two-body matrix elements $V_J^A(ab, cd)$ are given by

$$V_J^A(ab, cd) = [(1 + \delta_{ab})(1 + \delta_{cd})]^{-1/2}$$

$$\times \left[V_J(ab, cd) - (-1)^{j_c + j_d - J}V_J(ab, dc)\right] .$$ (3.8)

Before continuing discussion of the density decomposition, we note that the two-body Hamiltonian for fermion systems is completely specified by the set of antisymmetrized two-body matrix elements $V_J^A(ab, cd)$ that are the input to many standard shell model codes such as OXBASH [11]. Indeed, we can add to the $V_J^A(ab, cd)$ any set of (unphysical) symmetric two-body matrix elements $V_J^S(ab, cd)$ satisfying

$$V_J^S(ab, cd) = (-1)^{j_c + j_d - J}V_J^S(ab, dc) ,$$ (3.9)

without altering the action of $\hat{H}_2$ on any many-fermion wave function. However, note that although the

$V_J^S(ab, cd)$ do not alter the eigenstates and eigenvalues of the full Hamiltonian, they can (and do) affect the character of the decomposition of $\hat{H}_2$ into density operators, as is shown below. In what follows, we define the set of two-body matrix elements $V_J^N(ab, cd)$ that may possess no definite symmetries as

$$V_J^N(ab, cd) = V_J^A(ab, cd) + V_J^S(ab, cd) , \qquad (3.10)$$

allowing us to write the two-body Hamiltonian as

$$\hat{H}_2 = \frac{1}{4} \sum_{abcd} \sum_J [(1 + \delta_{ab})(1 + \delta_{cd})]^{1/2} V_J^N(ab, cd)$$
$$\times \sum_M A_{JM}^\dagger(ab) A_{JM}(cd) . \qquad (3.11)$$

To obtain the density decomposition of $\hat{H}_2$, we perform a Pandya transformation to recouple (a, c) and (b, d) into density operators with definite multipolarity,

$$\hat{\rho}_{KM}(ab) = \sum_{m_a, m_b} (j_a m_a j_b m_b | KM) a_{j_a m_a}^\dagger \tilde{a}_{j_b m_b} , \quad (3.12)$$

where $\tilde{a}_{j_a m_a} = (-1)^{j_a + m_a} a_{j_a m_a}$. Then $\hat{H}_2$ can be rewritten as

$$\hat{H}_2 = \hat{H}_2' + \hat{H}_1' , \qquad (3.13)$$

$$\hat{H}_2' = \frac{1}{2} \sum_{abcd} \sum_K E_K(ac, bd) \sum_M (-1)^M \hat{\rho}_{K-M}(ac) \hat{\rho}_{KM}(bd) , \qquad (3.14)$$

where the particle-hole matrix elements of the interaction are

$$E_K(ac, bd) = (-1)^{j_b + j_c} \sum_J (-1)^J (2J + 1) \begin{Bmatrix} j_a & j_b & J \\ j_d & j_c & K \end{Bmatrix}$$
$$\times \frac{1}{2} V_J^N(ab, cd) \sqrt{(1 + \delta_{ab})(1 + \delta_{cd})} \qquad (3.15)$$

and $\hat{H}_1'$ is a one-body operator given by

$$\hat{H}_1' = \sum_{ad} \epsilon_{ad}' \hat{\rho}_{0\,0}(a, d) , \qquad (3.16a)$$

with

$$\epsilon_{ad}' = -\frac{1}{4} \sum_b \sum_J (-1)^{J + j_a + j_b} (2J + 1) \frac{1}{\sqrt{2j_a + 1}}$$
$$\times V_J^N(ab, bd) \sqrt{(1 + \delta_{ab})(1 + \delta_{cd})} . \qquad (3.16b)$$

Note that adding symmetric matrix elements is equivalent to using the exchange decomposition for some parts of the interaction. The freedom in choosing the combinations of direct and exchange decomposition is then embodied in the arbitrary symmetric part of the matrix elements V_J^N.

Introducing the shorthand notation $i = (ac), j = (bd)$,

we can write Eq. (3.14) as

$$\hat{H}_2' = \frac{1}{2} \sum_{ij} \sum_K E_K(i, j)(-1)^M \hat{\rho}_{KM}(i) \hat{\rho}_{K-M}(j) . \quad (3.17)$$

Upon diagonalizing the matrix $E_K(i, j)$ to obtain eigenvalues $\lambda_{K\alpha}$ and associated eigenvectors $v_{K\alpha}$, we can represent $\hat{H}_2'$ as

$$\hat{H}_2' = \frac{1}{2} \sum_{K\alpha} \lambda_K(\alpha)(-1)^M \hat{\rho}_{KM}(\alpha) \hat{\rho}_{K-M}(\alpha) , \quad (3.18)$$

where

$$\hat{\rho}_{KM}(\alpha) = \sum_i \hat{\rho}_{KM}(i) v_{K\alpha}(i) . \qquad (3.19)$$

Finally, if we define

$$\hat{Q}_{KM}(\alpha) \equiv \frac{1}{\sqrt{2(1 + \delta_{M0})}}$$
$$\times [\hat{\rho}_{KM}(\alpha) + (-1)^M \hat{\rho}_{K-M}(\alpha)] , \quad (3.20a)$$

$$\hat{P}_{KM}(\alpha) \equiv -\frac{i}{\sqrt{2(1 + \delta_{M0})}}$$
$$\times [\hat{\rho}_{KM}(\alpha) - (-1)^M \hat{\rho}_{K-M}(\alpha)] , \quad (3.20b)$$

then $\hat{H}_2'$ becomes

$$\hat{H}_2' = \frac{1}{2} \sum_{K\alpha} \lambda_K(\alpha) \sum_{M \geq 0} [\hat{Q}_{KM}^2(\alpha) + \hat{P}_{KM}^2(\alpha)] . \quad (3.21)$$

This completes the representation of the two-body interaction as a diagonal quadratic form in density operators. We then couple auxiliary fields $\sigma_{KM}(\alpha)$ to $\hat{Q}_{KM}$ and $\tau_{KM}(\alpha)$ to $\hat{P}_{KM}$ in the HS transformation. (The latter are not to be confused with the "imaginary time" τ.)

In the treatment thus far, protons and neutrons were not distinguished from each other. Although the original Hamiltonian $\hat{H}_2$ conserves proton and neutron numbers, we ultimately might deal with one-body operators $\rho_{KM}(a_p, b_n)$ and $\rho_{KM}(a_n, b_p)$ (n,p subscripts denoting neutron and proton) that individually do not do so. The one-body Hamiltonian $\hat{h}_\sigma$ appearing in the HS transformation then mixes neutrons and protons. The single-particle wave functions in a Slater determinant then contain both neutron and proton components and neutron and proton numbers are not conserved separately in each Monte Carlo sample; rather the conservation is enforced only statistically.

It is, of course, possible to recouple so that only density operators separately conserving neutron and proton numbers $[\hat{\rho}_{KM}(a_p, b_p)$ and $\hat{\rho}_{KM}(a_n, b_n)]$ are present. To do so, we write the two-body Hamiltonian in a manifestly isospin-invariant form

$$\hat{H}_2 = \frac{1}{4} \sum_{abcd} \sum_J [(1 + \delta_{ab})(1 + \delta_{cd})]^{1/2} V_{JT}^N(ab, cd)$$
$$\times A_{JT;MT_z}^\dagger(ab) A_{JT;MT_z}(cd) , \qquad (3.22)$$

where, similar to the previous definition (3.6), the pair operator is

$$A^\dagger_{JT;MTz}(ab) = \sum_{m_a,m_b} (j_a m_a, j_b m_b | JM)$$

$$\times (\tfrac{1}{2}t_a, \tfrac{1}{2}t_b | TT_z) a^\dagger_{j_b m_b t_b} a^\dagger_{j_a m_a t_a} \; .$$

$$(3.23)$$

Here $(\tfrac{1}{2}, t_a)$, etc., are the isospin indices with $t_a = -\tfrac{1}{2}$ for proton states and $t_a = \tfrac{1}{2}$ for neutron states, and (TT_z) are the coupled isospin quantum numbers. The two-body Hamiltonian can now be written solely in terms of density operators that conserve the proton and neutron numbers. Namely,

$$\hat{H}_2 = \hat{H}'_1 + \hat{H}'_2 \; , \qquad (3.24)$$

where

$$\hat{H}'_1 = \sum_{ad} \sum_{t=p,n} \epsilon'_{ad} \rho_{0\,0,t}(a,d) \; , \qquad (3.25)$$

with

$$\epsilon'_{ad} = -\frac{1}{4} \sum_b \sum_J (-1)^{J+j_a+j_b} (2J+1) \frac{1}{\sqrt{2j_a+1}}$$

$$\times V^N_{J,T=1}(ab,bd)\sqrt{(1+\delta_{ab})(1+\delta_{cd})} \; ,$$

$$(3.26)$$

and

$$\hat{H}'_2 = \frac{1}{2} \sum_{abcd} \sum_{K,T=0,1} E_{KT}(ac,bd)[\hat{\rho}_{K,T}(i) \times \hat{\rho}_{K,T}(j)]^{J=0} \; .$$

$$(3.27)$$

Here, we define $\hat{\rho}_{KM,T}$ as

$$\hat{\rho}_{K\,M,T} = \hat{\rho}_{K\,M,p} + (-1)^T \hat{\rho}_{K\,M,n} \qquad (3.28)$$

and the $E_{K,T}$ are given by

$$E_{K,T=0}(ac,bd) = (-1)^{j_b+j_c} \sum_J (-1)^J (2J+1) \begin{Bmatrix} j_a & j_b & J \\ j_d & j_c & K \end{Bmatrix} \sqrt{(1+\delta_{ab})(1+\delta_{cd})}$$

$$\times \frac{1}{2} \left[V^N_{J,T=1}(ab,cd) + \frac{1}{2}[V^A_{J,T=0}(ab,cd) - V^S_{J,T=1}(ab,cd)] \right] \; , \qquad (3.29)$$

$$E_{K,T=1}(ac,bd) = -(-1)^{j_b+j_c} \sum_J (-1)^J (2J+1) \begin{Bmatrix} j_a & j_b & J \\ j_d & j_c & K \end{Bmatrix} \sqrt{(1+\delta_{ab})(1+\delta_{cd})}$$

$$\times \frac{1}{4} \left[V^A_{J,T=0}(ab,cd) - V^S_{J,T=1}(ab,cd) \right] \; . \qquad (3.30)$$

In this isospin formalism, since $A_{JT;MTz}(ab) = (-1)^{j_a+j_b-J+T} A_{JT;MTz}(ba)$, the definitions of the symmetric and antisymmetric parts of $V^N_{JT}(ab,cd)$, $V^S_{JT}(ab,cd)$, and $V^A_{JT}(ab,cd)$ become

$$V^{S/A}_{JT}(ab,cd) \equiv \frac{1}{2} \left[V^N_{JT}(ab,cd) \pm (-1)^{J+j_a+j_b+T-1} V^N_{JT}(ba,cd) \right] \; . \qquad (3.31)$$

Note that these expressions allow less freedom in manipulating the decomposition since we have to couple proton with proton and neutron with neutron in forming the density operators. Also note that $E_{K,T=0}(ac,bd) - E_{K,T=1}(ac,bd)$ is an invariant related only to the physical part of the interactions, $(V^A_{J,T=1} + V^A_{J,T=0})$. We can choose all $E_{K,T=1}$ to be zero in the above (by setting $V^S_{J,T=1} = V^A_{J,T=0}$) leaving $E_{K,T=0}$ completely determined by the physical matrix elements. In that case, we can halve the number of fields to be integrated. However, while introducing the isovector densities requires more fields, it also gives more freedom in choosing the unphysical matrix elements to optimize the calculation.

If we now diagonalize the $E_{KT}(i,j)$ as before and form the operators

$$\hat{Q}_{KM,T}(\alpha) \equiv \frac{1}{\sqrt{2(1+\delta_{M,0})}}$$

$$\times [\hat{\rho}_{KM,T}(\alpha) + (-1)^M \hat{\rho}_{K-M,T}(\alpha)] \; , \quad (3.32)$$

$$\hat{P}_{KM,T}(\alpha) \equiv -\frac{i}{\sqrt{2(1+\delta_{M,0})}}$$

$$\times [\hat{\rho}_{KM,T}(\alpha) - (-1)^M \hat{\rho}_{K-M,T}(\alpha)] \; , \quad (3.33)$$

the two-body part of the Hamiltonian can finally be written as

$$\hat{H}'_2 = \frac{1}{2} \sum_{KT} \sum_{\alpha} \lambda_{KT}(\alpha) \sum_{M \geq 0} \left[\hat{Q}^2_{K\,M,T}(\alpha) + \hat{P}^2_{K\,M,T}(\alpha) \right] . \tag{3.34}$$

In this decomposition, the one-body Hamiltonian $\hat{h}_{\sigma}$ of the HS transformation does not mix protons and neutrons. We can then represent the proton and neutron wave functions by separate determinants, and the number of neutrons and protons will be conserved rigorously during each Monte Carlo sample. For general interactions, even if we choose nonzero $E_{K,T=1}$ matrix elements, the number of fields involved is half that for the neutron-proton mixing decomposition, and the matrix dimension is also halved. These two factors combine to speed up the computation significantly. In this sense, an isospin formalism is more favorable, although at the cost of limiting the degrees of freedom embodied in the symmetric matrix elements V_J^S.

B. Pairing decomposition

In nuclei where the pairing interaction is important, it is natural to cast at least part of the two-body interaction as a quadratic form in pair creation and annihilation operators. We demonstrate this for the case where the Hamiltonian is written in the isospin formalism. Upon diagonalizing $V^A_{JT}(ab, cd)$ in Eq. (3.22), we can write

$$\hat{H}_2 = \sum_{JT\alpha} \lambda_{JT}(\alpha) \sum_{MT_z} A^{\dagger}_{JT;MT_z}(\alpha) A_{JT;MT_z}(\alpha) , \tag{3.35}$$

where

$$A^{\dagger}_{JT;MT_z}(\alpha) = \sum_i v_{JT\alpha}(i) A^{\dagger}_{JT,MT_z}(i) . \tag{3.36}$$

Separating $A^{\dagger}A$ into commutator and anticommutator terms, we have

$$\hat{H}_2 = \hat{H}'_2 + \hat{H}'_1 , \tag{3.37}$$

$$\hat{H}'_1 = \frac{1}{2} \sum_{JT\alpha} \lambda_{JT}(\alpha) \sum_{MT_z} \left[A^{\dagger}_{JT;MT_z}(\alpha), A_{JT;MT_z}(\alpha) \right] , \tag{3.38}$$

$$\hat{H}'_2 = \frac{1}{2} \sum_{JT\alpha} \lambda_{JT}(\alpha) \sum_{MT_z} \left\{ A_{JT;MT_z}(\alpha)^{\dagger}, A_{JT;MT_z}(\alpha) \right\} . \tag{3.39}$$

Clearly, $\hat{H}'_1$ is a one-body operator that can be combined with $\hat{H}_1$. The remaining two-body term can be written as a sum of squares by defining

$$Q_{JT;MT_z}(\alpha) \equiv \frac{1}{\sqrt{2}} [A^{\dagger}_{JT;MT_z}(\alpha) + A_{JT;MT_z}(\alpha)], \tag{3.40a}$$

$$P_{JT;MT_z}(\alpha) \equiv -\frac{i}{\sqrt{2}} [A^{\dagger}_{JT;MT_z}(\alpha) - A_{JT;MT_z}(\alpha)] , \tag{3.40b}$$

so that

$$\hat{H}'_2 = \frac{1}{2} \sum_{JT} \lambda_{JT}(\alpha) \sum_{MT_z} \left[Q^2_{JT;MT_z}(\alpha) + P^2_{JT;MT_z}(\alpha) \right] . \tag{3.41}$$

As in the density decomposition, we can then couple the σ and τ fields to Q and P, respectively.

Note that in the pairing decomposition, the one-body Hamiltonian $h(\tau)$ used in the path integral is a generalized one-body operator that includes density and pair creation and pair annihilation operators. The wave function is then propagated as a Hartree-Fock-Bogoliubov (HFB) state, rather than as a simple Slater determinant.

In this decomposition, neutrons and protons are inevitably mixed together in the one-body Hamiltonian $\hat{h}_{\sigma}$ (consider the Q,P terms for $T = 0$). In fact, $\hat{h}_{\sigma}$ also does not conserve the total number of nucleons; rather the conservation is only statistical after a large number of Monte Carlo samples.

For simplicity, we have described how to decompose the Hamiltonian solely in density operators or solely in pair operators. However, it is straightforward to mix the two decompositions with the choice depending on the type of interactions involved. Consider the "pairing plus quadrupole" model, namely,

$$\hat{H}_2 = -gP^{\dagger}P - \frac{1}{2}\chi Q \cdot Q , \tag{3.42}$$

where $P^{\dagger}, P$ are the monopole pair creation and annihilation operator and Q is the quadrupole-moment operator,

$$P^{\dagger} = \sum_{\alpha} a^{\dagger}_{\alpha} \tilde{a}^{\dagger}_{\alpha} , \tag{3.43}$$

$$Q_{\mu} = \sum_{\alpha\beta} \langle\alpha|Q_{\mu}|\beta\rangle \, a^{\dagger}_{\alpha} a_{\beta} . \tag{3.44}$$

Naively, it would be most convenient to use a pairing decomposition for the pairing interaction and a density decomposition for the quadrupole interaction. This would require only eight fields for each time slice in the HS transformation. The pure pairing or pure density decompositions would be much more complicated, as the former would require rewriting the quadrupole interactions in terms of pair operators and the latter would require rewriting the pairing interaction in terms of density operators. The numerical examples given in Sec. VI below will illustrate the behavior of such Hamiltonians under different decompositions.

IV. CALCULATION OF STATIC OBSERVABLES

In the previous sections, we expressed the evolution operator for a two-body Hamiltonian as a path integral over auxiliary fields in which the action involves only density

and pair operators. In this and the following section, we show how to extract observables from this path integral. The merit of this method will be clear from the compact formulas involved, which require handling only relatively small matrices of dimension N_s or $2N_s$, depending on the type of decomposition used. We derive formulas for three different approaches that use the evolution operator to obtain information about the system: the zero-temperature formalism, the grand-canonical ensemble, and the canonical ensemble. The zero-temperature and grand-canonical ensemble methods have been applied, with the density decomposition, to other physical systems such as the Hubbard model [6]. However, we believe that the canonical ensemble treatment presented here is novel.

The zero-temperature approach can be used only to extract ground-state information. On the other hand, the grand-canonical ensemble allows finite-temperature calculations, but fluctuations in particle number can be very significant in a system with a small number of nucleons. Thus, the canonical ensemble is particularly important in nuclear systems, where the particle number is small and shell structure is prominent. The grand-canonical ensemble yields information averaged over neighboring nuclei, which can have very different properties.

The canonical ensemble is more difficult than the other two approaches in two respects. First, the canonical (fixed-number) trace of U_σ is more difficult to compute than the wave function overlap of the zero-temperature formalism or the grand-canonical trace. Second, observables are more difficult to extract since Wick's theorem does not apply. We suggest two different methods to handle the canonical ensemble: the activity expansion and the integration over real coherent states. The coherent-state integration method can be applied to calculate canonical trace of any particle number involving only a negligible increase in computation time relative to the zero-temperature and grand-canonical approaches. Unfortunately, its utility is limited by the sign problem. On the other hand, the activity expansion, which is well suited (and numerically stable) for calculating nuclei with a small number of valence particles or holes, is less susceptible to the sign problem. (Yet a third method for extracting the canonical trace, based on Fourier analysis, shows good "sign" statistics and is numerically stable for midshell calculations; it is therefore suitable when the activity expansion fails. Details of this method will be published elsewhere [12].)

For each approach, we also derive the general formulas when pair operators (as well as density operators) are present in the single-particle Hamiltonian, i.e., when a pairing decomposition is used for some or all of the interaction. As far as we know, there are no known general formulas for the pairing decomposition formalism. Using the fermion coherent-state formalism [13], we derive in Appendix A a set of formulas for the calculation of observables that are similar to the well-known formulas for a pure density decomposition. Thus, our methods can be extended to calculations using general one-body operators in the HS transformation by only doubling the dimension of the matrices involved.

A. Zero-temperature formalism

We begin with "zero-temperature" observables. The trial wave function ψ_0 in Eq. (2.4) is, in principle, any state not orthogonal to the ground state. In practice, it is most conveniently a Slater determinant. If we have N_s m-scheme orbitals available and N_v indistinguishable particles, ψ_0 is constructed from N_v single-particle wave functions, each of which is a vector with N_s components, and we write ψ_0 as a Slater determinant of a $N_v \times N_s$ matrix, $\boldsymbol{\Psi}_0$.

In the pure density decomposition, consider the one-body Hamiltonian $\hat{h} = M_{ij} a_i^\dagger a_j$ (sums over the indices i, j from 1 to N_s are implicit). The evolved wave function

$$|\psi(\Delta\beta)\rangle = \exp(-\Delta\beta \hat{h})|\psi_0\rangle \qquad (4.1)$$

is then a Thouless transformation of the original determinant, the new state being represented by the matrix $\exp(-\Delta\beta M)\boldsymbol{\Psi}_0$. We can therefore represent the product of evolution operators by $N_s \times N_s$ matrices

$$\exp\left(-\Delta\beta \hat{h}_n\right) \cdots \exp\left(-\Delta\beta \hat{h}_1\right)$$

$$\rightarrow \exp\left(-\Delta\beta M_n\right) \cdots \exp\left(-\Delta\beta M_1\right) . \quad (4.2)$$

Let us now consider the overlap function in Eq. (2.16). Let $U_\sigma(\tau_2, \tau_1)$ be the matrix representing the evolution operator $\hat{U}_\sigma(\tau_2, \tau_1)$. Choosing some value τ of the imaginary time at which to insert the operator $\hat{O}$, we introduce the right and left wave functions $\psi_{R,L}(\tau)$ defined by

$$|\psi_R(\tau)\rangle = \hat{U}_\sigma(\tau, 0)|\psi_0\rangle , \qquad (4.3a)$$

$$|\psi_L(\tau)\rangle = \hat{U}_\sigma^\dagger(\beta, \tau)|\psi_0\rangle . \qquad (4.3b)$$

Then the required overlap in Eq. (2.16) is

$$\langle\psi_0|\hat{U}_\sigma(\beta, 0)|\psi_0\rangle = \langle\psi_L|\psi_R\rangle = \det\left[\boldsymbol{\Psi}_L^\dagger \boldsymbol{\Psi}_R\right] , \quad (4.4)$$

where

$$\boldsymbol{\Psi}_R(\tau) \equiv \mathbf{U}_\sigma(\tau, 0)\boldsymbol{\Psi}_0 , \quad \boldsymbol{\Psi}_L(\tau) \equiv \mathbf{U}_\sigma^\dagger(\beta, \tau)\boldsymbol{\Psi}_0 \quad (4.5)$$

are the matrices representing ψ_R and ψ_L. Note that if there are two distinguishable species of nucleons — protons and neutrons — and we use a decomposition that conserves the numbers of neutrons and protons, then there is a separate determinant for each set of single-particle wave functions and the total overlap is the product of the proton and neutron overlaps.

With the basic overlap in hand, we now turn to the expectation value of an operator $\hat{O}$ for a given field configuration [i.e., Eqs. (2.15) and (2.19)]. By Wick's theorem, the expectation value of any N-body operator can be expressed as the sum of products of expectation values of one-body operators. Hence, the basic quantity required is

$$\langle a_b^\dagger a_a\rangle_\sigma = \left[\boldsymbol{\Psi}_R\left(\boldsymbol{\Psi}_L^\dagger \boldsymbol{\Psi}_R\right)^{-1}\boldsymbol{\Psi}_L^\dagger\right]_{ba} . \qquad (4.6)$$

(A straightforward derivation of this expansion can be found in [14].) Again, when the decomposition separately conserves proton and neutron numbers, the expectation values for proton and neutron operators are given by separate matrices.

These formulas can be extended to the case where pair operators are present in the one-body Hamiltonian, i.e., when $\hat{h}$ is of the form

$$\hat{h} = \sum_{ij=1}^{N_s} (\Theta_{ij} a_i^\dagger a_j + \Delta_{ij} a_i^\dagger a_j^\dagger + \Lambda_{ij} a_i a_j) , \quad (4.7)$$

where Θ, Δ, and Λ are general $N_s \times N_s$ complex matrices. Our first task is to find a simple expression for $\langle\psi_0|\hat{U}_\sigma(\beta,0)|\psi_0\rangle$ where $\hat{U}_\sigma(\beta,0) = \prod_{n=1}^{N_t} \exp(-\Delta\beta\hat{h}_{\sigma_n})$. Using the fermion coherent-state representation and Grassman algebra, we derive the expressions in Appendix A. Here we simply state the results.

If the trial wave function ψ_0 is a quasiparticle vacuum, such that $\beta_i|\psi_0\rangle = 0$ where $\beta_i = \sum_j u_{ij} a_j + v_{ij} a_j^\dagger$, then

$$\langle\psi_0|\prod_{n=1}^{N_t} \exp(-\Delta\beta\hat{h}_n)|\psi_0\rangle$$

$$= \det\left[(v^* \quad u^*) \, U_\sigma(\beta,0) \begin{pmatrix} v^T \\ u^T \end{pmatrix} \right]^{\frac{1}{2}}$$
$$\times \exp\left(-\frac{\Delta\beta}{2}\sum_{n=1}^{N_t} \text{Tr}[\Theta_n]\right) , \quad (4.8)$$

where

$$U_\sigma(\beta,0) = \exp(-\Delta\beta M_{N_t})\cdots\exp(-\Delta\beta M_1) \quad (4.9)$$

is the matrix representing the evolution operator $\hat{U}_\sigma(\beta,0)$, and M_n is the $2N_s \times 2N_s$ matrix representing $\hat{h}_n$:

$$M_n = \begin{pmatrix} \Theta_n & \Delta_n - \Delta_n^T \\ \Lambda_n - \Lambda_n^T & -\Theta_n^T \end{pmatrix} . \quad (4.10)$$

Here, the evolution operator $\hat{U}_\sigma(\tau_2,\tau_1)$ is represented by a $2N_s \times 2N_s$ matrix and the many-body wave function is represented by a $2N_s \times N_s$ matrix, independent of the number of particles present. In analogy to Eqs. (4.3–4.6), we can write

$$\langle\psi_0|\hat{U}_\sigma(\beta,0)|\psi_0\rangle = \langle\psi_L|\psi_R\rangle$$
$$= \det\left[\Psi_L^\dagger \Psi_R\right]^{\frac{1}{2}}$$
$$\times \exp\left(-\frac{\Delta\beta}{2}\sum_{n=1}^{N_t} \text{Tr}[\Theta_n]\right) , \quad (4.11)$$

where

$$\Psi_R \equiv U_\sigma(\tau,0) \begin{pmatrix} v^T \\ u^T \end{pmatrix}, \quad \Psi_L \equiv U_\sigma^\dagger(\beta,\tau) \begin{pmatrix} v^T \\ u^T \end{pmatrix} . \quad (4.12)$$

To calculate the expectation value of a generalized one-body operator, we proceed as in the pure density case. Let

$$\alpha_i = a_i, \quad i = 1,\ldots,N_s , \quad (4.13a)$$

$$\alpha_{i+N_s} = a_i^\dagger, \quad i = 1,\ldots,N_s . \quad (4.13b)$$

Then the one-quasiparticle density matrix is

$$\langle\alpha_a^\dagger \alpha_b\rangle_\sigma = \frac{\langle\psi_L|\hat{\rho}_{ab}|\psi_R\rangle}{\langle\psi_L|\psi_R\rangle} = \frac{1}{2}\left[\Psi_R(\Psi_L^\dagger\Psi_R)^{-1}\Psi_L^\dagger\right]_{ba} - \frac{1}{2}\left[\begin{pmatrix}0&1\\1&0\end{pmatrix}\Psi_R(\Psi_L^\dagger\Psi_R)^{-1}\Psi_L^\dagger\begin{pmatrix}0&1\\1&0\end{pmatrix}\right]_{ab} + \delta_{ab}$$
$$= \left[\Psi_R(\Psi_L^\dagger\Psi_R)^{-1}\Psi_L^\dagger\right]_{ba} . \quad (4.14)$$

The final step follows from the properties of **U** in Eq. (A20). Note that both the overlap and the Green's function are similar to those of the density decomposition. However, the enlarged dimension of the representation matrices causes the overlap to be the square root of a determinant rather than just a determinant. We know of no simple way to determine the sign of the square root. Computationally, it can be traced by watching the evolution of $\langle\psi_0|\hat{U}_\sigma(\tau,0)|\psi_0\rangle$ as $\hat{U}_\sigma$ is built up from 0 to β (Appendix B), although at the expense of increased computation. Also, the linear dimension of the matrix used in the calculation is twice that for the pure density decomposition case so that the pairing decomposition is more computationally demanding. However, when the interaction has a strong pairing character, it has the po-

tential for a more effective Monte Carlo sampling, and offers greater freedom in the decomposition, which might be used to mitigate the sign problem.

B. Grand-canonical ensemble

For the grand-canonical ensemble, the trace in Eq. (2.18) is a sum over all possible many-body states with all possible nucleon numbers, and a chemical potential in $\hat{H}$ is required. For the pure density decomposition, the many-body trace is given by

$$\zeta(\sigma) = \hat{\text{Tr}}\,\hat{U}_\sigma(\beta,0) = \det\left[1 + U_\sigma(\beta,0)\right] , \quad (4.15)$$

which can be proved by expanding the determinant [14].

For the expectation value of a one-body operator, one can recapitulate exactly the argument of the zero-temperature development and obtain

$$\langle a_a^\dagger a_b \rangle_\sigma = \{[1 + \mathbf{U}_\sigma(\beta,0)]^{-1}\,\mathbf{U}_\sigma(\beta,0)\}_{ba}\ . \qquad (4.16)$$

We have extended these formulas to decompositions that involve pairing operators (Appendix A). The results are given in terms of the $2N_s \times 2N_s$ matrices $\mathbf{M}_n$, $\mathbf{U}(\beta,0)$ representing the Hamiltonians $\hat{h}_n$ and the evolution operator $\hat{U}(\beta,0)$, [Eqs. (4.9 and 4.10)] namely,

$$\hat{\mathrm{Tr}}\left[\hat{U}(\beta,0)\right] = \det\left[1 + \mathbf{U}(\beta,0)\right]^{\frac{1}{2}} \exp\left(-\frac{\Delta\beta}{2}\mathrm{Tr}[\Theta_n]\right)\ . \qquad (4.17)$$

To motivate this formula, consider the simplest case of one time slice where $\hat{U} = \exp(-\hat{h})$ and $\hat{h}$ is Hermitian and in the form (4.7). Then, $\hat{h}$ can be diagonalized by a HFB transformation

$$\hat{h} = \frac{1}{2}\begin{pmatrix} a^\dagger & a \end{pmatrix}\begin{pmatrix} \Theta & \Delta - \Delta^T \\ \Lambda - \Lambda^T & -\Theta^T \end{pmatrix}\begin{pmatrix} a \\ a^\dagger \end{pmatrix} + \frac{1}{2}\mathrm{Tr}[\Theta]$$

$$= \sum_i e_i \beta_i^\dagger \beta_i - \frac{1}{2}e_i + \frac{1}{2}\mathrm{Tr}[\Theta]\ , \qquad (4.18)$$

where

$$\begin{pmatrix} \beta \\ \beta^\dagger \end{pmatrix} = \begin{pmatrix} u & v^* \\ v & u^* \end{pmatrix}\begin{pmatrix} a \\ a^\dagger \end{pmatrix} \qquad (4.19)$$

and

$$\begin{pmatrix} u & v^* \\ v & u^* \end{pmatrix}\begin{pmatrix} \Theta & \Delta - \Delta^T \\ \Lambda - \Lambda^T & -\Theta^T \end{pmatrix}\begin{pmatrix} u^\dagger & v^\dagger \\ v^T & u^T \end{pmatrix}$$

$$= \begin{pmatrix} \epsilon_1 & 0 & \dots & 0 & 0 & \dots \\ 0 & \epsilon_2 & \dots & 0 & 0 & \dots \\ \vdots & \vdots & \ddots & \vdots & \vdots & \ddots \\ 0 & 0 & \dots & -\epsilon_1 & 0 & \dots \\ 0 & 0 & \dots & 0 & -\epsilon_2 & \dots \\ \vdots & \vdots & \ddots & \vdots & \vdots & \ddots \end{pmatrix}\ . \qquad (4.20)$$

In the diagonal form, $\hat{\mathrm{Tr}}[\exp(-\hat{h})]$ can be identified easily as

$$\prod_i [(1 + e^{-\epsilon_i})e^{\frac{1}{2}\epsilon_i}]e^{-\frac{1}{2}\mathrm{Tr}[\Theta]}$$

$$= \prod_i \sqrt{(1 + e^{-\epsilon_i})(1 + e^{\epsilon_i})}e^{-\frac{1}{2}\mathrm{Tr}[\Theta]}$$

$$= \det[(1 + e^{-M})^{\frac{1}{2}}]e^{-\frac{1}{2}\mathrm{Tr}[\Theta]}\ , \qquad (4.21)$$

due to the invariance of the determinant with respect to similarity transformations. Here, as in the overlap formulae for zero-temperature approach, the grand-canonical trace is given as the square root of a determinant, so that the evolution of the sign is important (Appendix B). The formula for the observables can be calculated from

$$\langle \alpha_a^\dagger \alpha_b \rangle_\sigma = \frac{1}{2}\left\{[(1 + \mathbf{U}(\beta,0))^{-1}\,\mathbf{U}(\beta,0)]\right\}_{ba} - \frac{1}{2}\left[\begin{pmatrix} \mathbf{0} & \mathbf{1} \\ \mathbf{1} & \mathbf{0} \end{pmatrix}[1 + \mathbf{U}(\beta,0)]^{-1}\mathbf{U}(\beta,0)\begin{pmatrix} \mathbf{0} & \mathbf{1} \\ \mathbf{1} & \mathbf{0} \end{pmatrix}\right]_{ab} + \frac{1}{2}\delta_{ab}$$

$$= \left\{[1 + \mathbf{U}(\beta,0)]^{-1}\mathbf{U}(\beta,0)\right\}_{ba}\ . \qquad (4.22)$$

C. Activity expansion for the canonical ensemble

As mentioned in the beginning of this section, the grand-canonical ensemble may lead to large fluctuations in the particle number for systems with few particles, and so is particularly ill suited for small nuclear systems, and although the particle number does not fluctuate in the zero-temperature approach, that formalism can only give ground-state results. The canonical ensemble is therefore important for studying thermal behavior, as well as the ground state of large systems.

In the canonical ensemble, we have to find the trace of $\hat{U}_\sigma(\beta,0)$ over all states with a fixed particle number N_v (actually fixed proton and neutron numbers). We discuss two methods of achieving this: the activity expansion presented here and the integration over real coherent states presented in the following subsection.

Consider first the case when only density operators are present in the one-body Hamiltonian $\hat{h}$. From the grand-canonical ensemble formulas (4.15), one can see that the canonical trace is just the sum of all the $N_v \times N_v$ sub-determinants. More explicitly, we consider the *activity expansion*: For some parameter λ, let

$$Z(\beta,\lambda) = \hat{\mathrm{Tr}}\lambda^{\hat{N}_v}e^{-\beta\hat{H}} = \sum_{N_v} \lambda^{N_v}\,Z_{N_v}(\beta)\ . \qquad (4.23)$$

In our matrix representation,

$$\hat{\mathrm{Tr}}\,\lambda^{\hat{N}}\hat{U}_\sigma(\beta,0) = \det(1 + \lambda\mathbf{U})\ . \qquad (4.24)$$

If Eq. (4.24) is expanded in powers of λ, the coefficient of λ^{N_v} is just the canonical trace of $\hat{U}_\sigma(\beta,0)$ over N_v particles, so that $\det(1 + \lambda\mathbf{U})$ is the generating function for the canonical trace. Thus,

$$Z_{N_v}(\beta) = \int \mathcal{D}[\sigma] G(\sigma) \zeta_{N_v}(\sigma) , \qquad (4.25)$$

where

$$\det[1 + \lambda \mathbf{U}_\sigma(\beta, 0)] = \sum_{N_v} \lambda^{N_v} \zeta_{N_v}(\sigma) . \qquad (4.26)$$

The trick now is to find simpler expressions for ζ_{N_v}, instead of doing the explicit sum over the determinants. To do this, write

$$\det(1 + \lambda \mathbf{U}) = \exp \mathrm{Tr} \ln(1 + \lambda \mathbf{U})$$

$$= \exp \left(\sum_{n=1}^{\infty} \frac{(-1)^{n-1}}{n} \lambda^n \mathrm{Tr}\,[\mathbf{U}^n] \right) . \qquad (4.27)$$

This expansion converges to the generating function because $Z(\beta, \lambda)$ is a polynomial in λ of finite order (i.e., N_v

can be at most N_s). The coefficient of λ^n in the exponential is readily found. For a given particle number N_v, we need only calculate matrix traces up to $\mathrm{Tr}[\mathbf{U}^{N_v}]$ and the coefficient of λ^{N_v} can be extracted accordingly.

For one-body expectation values, using again the grand-canonical trace as the generating function for calculating observables and collecting all terms with coefficient λ^{N_v}, we arrive at

$$\left\langle a_a^\dagger a_b \right\rangle_{\sigma, N_v} = \sum_{n=1}^{N_v} (-1)^{n-1} \left(\mathbf{U}^n\right)_{ba} \zeta_{N-n}(\sigma)/\zeta_N(\sigma) . \qquad (4.28)$$

The expectation value of two-body operators, $\langle \rho_{ab} \rho_{cd}(\sigma) \rangle_{N_v}$, is nontrivial as Wick's theorem must be modified, but again one can simply collect the terms with coefficient λ^{N_v} and obtain

$$\left\langle a_a^\dagger a_b a_c^\dagger a_d \right\rangle_{\sigma, N_v} = \sum_{n=1}^{N_v} \left\{ \sum_{m=1}^{N_v} \left[(-1)^{m+n} \left(\mathbf{U}_{ba}^n \mathbf{U}_{dc}^m - \mathbf{U}_{da}^n \mathbf{U}_{bc}^m \right) \zeta_{N_v - m - n}(\sigma)/\zeta_{N_v}(\sigma) \right] \right. $$

$$\left. + \delta_{bc}(-1)^{N_v - 1} \mathbf{U}_{da}^n \zeta_{N_v - n}(\sigma)/\zeta_{N_v}(\sigma) \right\} . \qquad (4.29)$$

This form of the activity expansion works best for $N_v \leq N_s/2$ (mostly empty model spaces). When $N_v > N_s/2$ (mostly filled spaces), it is more efficient to expand in the activity of the hole states. In this case, we define

$$Z_\sigma(\beta, \lambda) = \hat{\mathrm{Tr}}[\lambda^{N_s - \hat{N}} e^{-\beta \hat{H}}] , \qquad (4.30)$$

and, as in Eq. (4.24),

$$\hat{\mathrm{Tr}}[\lambda^{N_s - \hat{N}} \hat{U}(\beta, 0; \sigma)] = \det[\lambda + \mathbf{U}] . \qquad (4.31)$$

The coefficient of λ^N is the partition function for N holes,

$$\det[\lambda + \mathbf{U}] = \det[\mathbf{U}] \exp \left(\sum_{n \geq 1} \frac{1}{n} (-1)^{n-1} \lambda^n \mathrm{Tr}[\mathbf{U}^{-n}] \right) \equiv \sum_N \lambda^N \zeta_N' , \qquad (4.32)$$

the expectation value of a one-body operator is

$$\langle \rho_{ij} \rangle_{N \text{ holes}} = \sum_{n=0}^{N} (-1)^n \mathbf{U}_{ji}^{-n} \zeta_{N-n}'/\zeta_N' , \qquad (4.33)$$

and the expectation of a two-body operator is

$$\langle \rho_{ij} \rho_{kl} \rangle_{N \text{ holes}} = \sum_{n=0}^{N} \delta_{jk}(-1)^n \mathbf{U}_{li}^{-n} \zeta_{N-n}'/\zeta_N') + \left(\sum_{m=0}^{N} (-1)^{m+n} (\mathbf{U}_{ji}^{-n} \mathbf{U}_{lk}^{-m} - \mathbf{U}_{li}^{-n} \mathbf{U}_{jk}^{-m}) \right) \zeta_{N-m-n}'/\zeta_N' . \qquad (4.34)$$

When pairing operators are involved, we use Eq. (4.17) for the grand-canonical trace, which becomes the generating function for the corresponding canonical trace. As an illustration, we display the formula for the expansion in particle activity,

$$\hat{\mathrm{Tr}}\left[\lambda^{\hat{N}}\hat{U}\right] = \det\left[\begin{pmatrix} 1 & 0 \\ 0 & 1 \end{pmatrix} + \begin{pmatrix} \lambda\mathbf{1} & 0 \\ 0 & \frac{1}{\lambda}\mathbf{1} \end{pmatrix}\mathbf{U}\right]^{\frac{1}{2}}\lambda^{\frac{N_s}{2}}$$

$$= \det\left[\begin{pmatrix} 1 & 0 \\ 0 & 1 \end{pmatrix} + \begin{pmatrix} \lambda\mathbf{1} & 0 \\ 0 & \frac{1}{\lambda}\mathbf{1} \end{pmatrix}\begin{pmatrix} \mathbf{S}^{11} & \mathbf{S}^{12} \\ \mathbf{S}^{12} & \mathbf{S}^{22} \end{pmatrix}\right]^{\frac{1}{2}}\lambda^{\frac{N_s}{2}}$$

$$= \det\left[\begin{pmatrix} 1 & \mathbf{S}^{12} \\ 0 & \mathbf{S}^{22} \end{pmatrix}\right]^{\frac{1}{2}}\det\left[\begin{pmatrix} 1 & 0 \\ 0 & 1 \end{pmatrix} + \lambda\begin{pmatrix} 1 & \mathbf{S}^{12} \\ 0 & \mathbf{S}^{22} \end{pmatrix}^{-1}\begin{pmatrix} \mathbf{S}^{11} & 0 \\ \mathbf{S}^{12} & 1 \end{pmatrix}\right]^{\frac{1}{2}}$$

$$= \det\left[\begin{pmatrix} 1 & \mathbf{S}^{12} \\ 0 & \mathbf{S}^{22} \end{pmatrix}\right]^{\frac{1}{2}}\exp\left(\frac{1}{2}\mathrm{Tr}\left\{\ln\left[\begin{pmatrix} 1 & 0 \\ 0 & 1 \end{pmatrix} + \lambda\mathbf{Y}\right]\right\}\right)$$

$$= \det\left[\mathbf{S}^{22}\right]^{\frac{1}{2}}\exp\left(\frac{1}{2}\sum_n \mathrm{Tr}\left[\mathbf{Y}^n\right](-1)^{n-1}\frac{\lambda^n}{n}\right), \qquad (4.35)$$

where the definitions of $\mathbf{S}^{11}, \mathbf{S}^{12}, \mathbf{S}^{21}, \mathbf{S}^{22}$ are obvious, and

$$\mathbf{Y} \equiv \begin{pmatrix} 1 & \mathbf{S}^{12} \\ 0 & \mathbf{S}^{22} \end{pmatrix}^{-1}\begin{pmatrix} \mathbf{S}^{11} & 0 \\ \mathbf{S}^{12} & 1 \end{pmatrix}. \qquad (4.36)$$

The expectation values of one- and two-body operators can then be derived as in the pure density decomposition.

D. Canonical ensemble via coherent states

We make use of the operator

$$\hat{J} = C\int\prod_{ph}dX_{ph}\frac{|X\rangle\langle X|}{\det(1 + X^T X)^{\frac{N_s}{2}+1}}, \qquad (4.37)$$

which can be shown [15] to be a resolution of unity in the Hilbert space of N_v fermions occupying N_s levels. Here, X_{ph} are the real integration variables, $|X\rangle$ are the real coherent states,

$$|X\rangle = \exp\left(\sum_{hp}X_{ph}a_p^\dagger a_h\right)|0\rangle,$$

$$h = 1,\ldots,N_v, \quad p = N_v + 1,\ldots,N_s, \quad (4.38)$$

$|0\rangle$ is the N_v-fermion state with the levels $1,\ldots,N_v$ occupied, and C is a normalization constant,

$$C = \prod_{p=N_v+1}^{N_s} C_p, \qquad (4.39)$$

$$C_p = \pi^{-N_s/2}\Gamma\left(\frac{p}{2}+1\right)\bigg/\Gamma\left(\frac{p - N_v}{2}+1\right).$$

The canonical trace can then be cast in a form of expectation with integration over the variables X_{ph}. For any operator $\hat{O}$,

$$\hat{\mathrm{Tr}}[\hat{O}] = C\int dX\frac{\langle X|\hat{O}|X\rangle}{\det(1 + X^T X)^{\frac{N_s}{2}+1}}, \qquad (4.40)$$

where $dX = \prod_{ph}dX_{ph}$. The thermal canonical expectation is then

$$\langle\hat{O}\rangle = \frac{\hat{\mathrm{Tr}}[\hat{O}e^{-\beta\hat{H}}]}{\hat{\mathrm{Tr}}[e^{-\beta\hat{H}}]} = \frac{\int\mathcal{D}[\sigma]G(\sigma)dX\langle X|\hat{U}_\sigma(\beta,0)\hat{O}|X\rangle/\det(1 + X^T X)^{N_s/2+1}}{\int\mathcal{D}[\sigma]G(\sigma)dX\langle X|\hat{U}_\sigma(\beta,0)|X\rangle/\det(1 + X^T X)^{N_s/2+1}}. \qquad (4.41)$$

We can compute the overlap and the observable in (4.41) as in the zero-temperature formalism, but we now have to do the Monte Carlo integration over the fields X_{ph} as well. However, the number of these fields scales only as N_s^2, which is about the same as the number of σ fields in one time slice, so that introducing the coherent-state integration is not much more computationally expensive than the zero-temperature formalism. The advantage of coherent states is that we do not have to find

$\mathrm{Tr}[\mathbf{U}(\beta,0)^n]$. However, the integration of the coherent states may aggravate the sign problem, as will be discussed in Secs. VI and VII.

V. DYNAMICAL CORRELATIONS

In the previous section, we discussed how to extract the expectation value of a one-body operator $\langle\hat{O}\rangle$ and, by

use of Wick's theorem and its extension to the canonical case, equal-time two-body operators $\langle \hat{A}\hat{B} \rangle$, etc. A great deal of the interesting physics, however, is contained in the dynamical response function $\langle \hat{O}^\dagger(t)\hat{O}(0) \rangle$ where $\hat{O}(t) = e^{-i\hat{H}t}\hat{O}e^{i\hat{H}t}$. In our calculations, we evaluate the imaginary-time response function $\langle \hat{O}^\dagger(i\tau)\hat{O}(0) \rangle$ and from it deduce the associated strength function, $f_{\hat{O}}(E)$.

In the zero-temperature formalism, the strength function is

$$f_{\hat{O}}(E) \equiv \sum_f \delta(E - E_f + E_i)|\langle f|\hat{O}|i \rangle|^2 , \qquad (5.1)$$

where i is the ground state, while in the canonical or grand-canonical ensemble,

$$f_{\hat{O}}(E) \equiv \frac{1}{Z} \sum_{i,f} \delta(E - E_f + E_i)e^{-\beta E_i}|\langle f|\hat{O}|i \rangle|^2 . \qquad (5.2)$$

Thus, the imaginary-time response function is related to the strength function by a Laplace transform,

$$R(\tau) \equiv \langle \hat{O}^\dagger(i\tau)\hat{O}(0) \rangle = \int_{-\infty}^{\infty} f_{\hat{O}}(E)e^{-\tau E}dE . \qquad (5.3)$$

Recovering the strength function from R by inversion of the Laplace transform is an ill-posed numerical problem. Different methods have been proposed to surmount this difficulty [16,17]. We resort to making the best "guess" for the strength function via the classic maximum entropy (ME) method [18,19], which was first introduced to recover strength functions in Monte Carlo calculations by Silver et al. [17] and has since been widely used in similar condensed matter simulations. It is in essence a least-squares fit biased by a measure of the phase space of the strength function.

In ME methods, the function to be minimized is $\frac{1}{2}\chi^2 - \alpha S$, where χ^2 is the usual square of the residuals, S is the entropy of the phase space (not to be confused with the action in the auxiliary field path integral), and α is a Lagrange multiplier. In classic ME α is determined self-consistently. The method, described briefly in Appendix C, also can yield error estimates for the extracted strength function.

To calculate the imaginary-time response, consider $\left\langle \hat{A}(i\tau)\hat{B}(0) \right\rangle$ and write the thermal expectation as a path integral:

$$\langle \hat{A}(i\tau)\hat{B}(0) \rangle$$

$$= \frac{\hat{\mathrm{Tr}}[e^{-(\beta-\tau)\hat{H}}\hat{A}e^{-\tau\hat{H}}\hat{B}]}{\hat{\mathrm{Tr}}[e^{-\beta\hat{H}}]}$$

$$= \frac{\int \mathcal{D}[\sigma]G(\sigma)\hat{\mathrm{Tr}}[\hat{U}_\sigma(\beta,0)]\frac{\hat{\mathrm{Tr}}[\hat{U}_\sigma(\beta,\tau)\hat{A}\hat{U}_\sigma(\tau,0)\hat{B}]}{\hat{\mathrm{Tr}}[\hat{U}_\sigma(\beta,0)]}}{\int \mathcal{D}[\sigma]G(\sigma)\hat{\mathrm{Tr}}[\hat{U}_\sigma(\beta,0)]} . \qquad (5.4)$$

Upon defining

$$\hat{O}_\sigma(\tau) \equiv \hat{U}_\sigma(\tau,0)^{-1}\hat{O}\hat{U}_\sigma(\tau,0) , \qquad (5.5)$$

we have an expression suitable for Monte Carlo evaluation,

$$\langle \hat{A}(i\tau)\hat{B}(0) \rangle$$

$$= \frac{\int \mathcal{D}[\sigma]G(\sigma)\hat{\mathrm{Tr}}[\hat{U}_\sigma(\beta,0)]\frac{\hat{\mathrm{Tr}}[\hat{U}_\sigma(\beta,0)\hat{A}_\sigma(\tau)\hat{B}_\sigma(0)]}{\hat{\mathrm{Tr}}[\hat{U}_\sigma(\beta,0)]}}{\int \mathcal{D}[\sigma]G(\sigma)\hat{\mathrm{Tr}}[\hat{U}_\sigma(\beta,0)]} \qquad (5.6a)$$

$$= \frac{\int \mathcal{D}[\sigma]e^{-\mathcal{S}(\sigma)}\langle \hat{A}_\sigma(\tau)\hat{B}_\sigma(0) \rangle}{\int \mathcal{D}[\sigma]e^{-\mathcal{S}(\sigma)}} . \qquad (5.6b)$$

We now proceed to find $\hat{O}_\sigma(\tau)$. For the purpose of illustration, we show the formulas for the pure density decomposition (formulas for the general case can be derived similarly). For the simplest case when $\hat{O} = a_i^\dagger$ or $\hat{O} = a_i$, it can be shown that [14]

$$a_{i\,\sigma}^\dagger(n\Delta\beta) = \sum_j [\mathbf{U}_\sigma(n\Delta\beta,0)^{-1}]_{ij}^T a_j^\dagger , \qquad (5.7a)$$

$$a_{i\sigma}(n\Delta\beta) = \sum_j \mathbf{U}_\sigma(n\Delta\beta,0)_{ij}a_j . \qquad (5.7b)$$

In this way, the creation and annihilation operators can be "propagated" back to $\tau = 0$. Any operator $\hat{O}_\sigma(\tau)$ can be first expressed in $a_\sigma(\tau)$ and $a^\dagger_\sigma(\tau)$ and therefore can be propagated back and expressed in a and $a^\dagger$. For example, suppose $\hat{O} = C_{ij}a_i^\dagger a_j$ is a one-body operator. Then

$$\hat{O}_\sigma(\tau) = \hat{U}_\sigma(\tau,0)^{-1}\hat{O}\hat{U}_\sigma(\tau,0) \qquad (5.8)$$

$$= [\mathbf{U}_\sigma(\tau,0)^{-1}\mathbf{C}\mathbf{U}_\sigma(\tau,0)]_{ij}a_i^\dagger a_j . \qquad (5.9)$$

Thus, the response function can be measured in the same way as the static observables.

VI. COMPUTATIONAL DETAILS AND ILLUSTRATIONS

A. Monte Carlo methods

Monte Carlo evaluation of the path integral requires a weight function. We have tried two different choices for the weight function, each with advantages and disadvantages.

One choice for the weight function is a Gaussian, with the the static mean-field solution as the centroid, and the widths given by the random phase approximation (RPA) frequencies. Thus, much of the known physics is embodied in the weight and the Monte Carlo evaluates corrections to the mean-field + RPA approximation. Further, it is simple to efficiently generate random field configurations with a Gaussian distribution.

Unfortunately, Gaussian sampling has several disadvantages. First, finding the RPA frequencies can be extremely time consuming since we have to calculate and diagonalize the curvature matrix $\frac{\partial^2}{\partial\sigma_{\alpha,i}\partial\sigma_{\gamma,j}}\frac{\partial^2 \mathcal{S}}{\partial\sigma\partial\sigma}$ at the mean-field solution. (Here, α,γ run through the number of quadratic terms in the Hamiltonian and i,j run through the number of time slices.) For any general in-

teraction, the curvature matrix has a large dimension, $N_s^2 N_t$. Second, the Gaussian has to be modified when there is spontaneous symmetry breaking in the mean fields (such as quadrupole deformation). Otherwise, the Goldstone modes in the the RPA frequencies (e.g., zero eigenvalues corresponding to shape rotations) will destroy the normalizability of the weight function. Finally, multiple mean-field solutions well separated from each other can also pose a problem, so that multiple Gaussians may be needed.

A more satisfactory route is to choose $|\exp(-\mathcal{S})| = G(\sigma)|\zeta(\hat{U}_\sigma(\beta, 0))|$ as the weight function and to use a stochastic random walk such as the Metropolis algorithm to generate the fields. The expectation of an observable is then given by Eq. (2.21) where

$$\Phi_i = \exp[-i\operatorname{Im}(\mathcal{S}_i)] . \tag{6.1}$$

The Metropolis algorithm is free of the disadvantages for the Gaussian weight function, in that it will eventually sample the entire space where $|\exp(-\mathcal{S})|$ is significant. The main disadvantages of Metropolis are its inefficiency as currently implemented and the "sign problem." Let us define the denominator of Eq. (2.21) by $\langle\Phi\rangle$:

$$\langle\Phi\rangle \equiv \frac{1}{N}\sum_i \exp[-i\operatorname{Im}(\mathcal{S}_i)] . \tag{6.2}$$

If $\langle\Phi\rangle \ll 1$, the large fluctuations defeat any attempt at a Monte Carlo evaluation. This "sign problem" will be addressed in detail in the examples illustrated below.

For the Metropolis algorithm, we take random steps in the fields time slice by time slice, following a sweeping procedure introduced by Koonin et al. [4]. For the Monte Carlo results to be valid, one requires that the points in the random walk be both distributed as the weight function and be statistically independent. The first requirement translates into starting the fields in a region of statistically significant weight; if the initial configuration has a small weight, a number of initial "thermalization" sweeps are usually needed to relax the fields to this region. The second requirement means that the walker must sweep through the fields many times to decorrelate the samples.

The number of thermalization sweeps and decorrelation sweeps increases with system size, and the choice of random walk procedure greatly affects the sampling efficiency. In the early stage of investigation, we allowed all fields σ_α at one time slice to change with equal probability within a certain step size. The acceptance is then determined by the ratio of the weight $|\exp(-\mathcal{S})|$ of the old and new configurations, and we adjusted the step size to give an average acceptance probability of 0.5. The calculations of sd-shell nuclei described below then needed approximately 2000 thermalization sweeps and up to 200 decorrelation sweeps between samples. In our later work, we used another random walk algorithm, in which a fixed number of fields at one time slice are randomly chosen for updating; those chosen are generated from the Gaussian distribution in Eq. (2.9b) while the others are kept at their previous values, and the acceptance is determined

by the ratio of ζ in the new and old configurations. This alternative algorithm needs only some 200 thermalization sweeps and 10 decorrelation sweeps; i.e., it is 10 times more efficient than the previous method. In addition, boundaries where $|\exp(-\mathcal{S})| = 0$ can confine the first random walk algorithm, while they do not affect the second.

The random walk can thermalize faster if it starts from a configuration where the weight $W(\sigma)$ is large. Usually we start from the static mean fields, given by

$$\sigma_{\alpha,n} = \bar{\sigma}_\alpha, \quad n = 1, N_t , \tag{6.3a}$$

$$\bar{\sigma}_\alpha = -s_\alpha \operatorname{sgn}(V_\alpha)\langle\hat{O}_\alpha\rangle_{\bar{\sigma}} . \tag{6.3b}$$

One can show that for canonical and grand-canonical calculations, the static mean field $\bar{\sigma}_\alpha$ is a saddle point of the weight function,

$$\left.\frac{\partial[G(\sigma)\zeta(\sigma)]}{\partial\sigma_{\alpha,i}}\right|_{\bar{\sigma}} = 0 . \tag{6.4}$$

For the zero-temperature approach, we also choose the self-consistent field solution $\bar{\sigma}_\alpha$, although Eq. (6.4) is not rigorously satisfied. This is preferable to starting the fields at zero, which may be far from configurations of significant weight.

The mean-field solution (6.3) can be found iteratively,

$$\{\bar{\sigma}_\alpha\}_{i+1} = -s_\alpha \operatorname{sgn}(V_\alpha)\langle\hat{O}_\alpha\rangle_{\bar{\sigma}_i} . \tag{6.5}$$

For the systems we have tested, Eq. (6.5) usually converges within 100 interactions starting from $\bar{\sigma}_\sigma = 0$. For larger systems and at lower temperature, convergence is slow and sometimes unstable or barely stable. In that case taking

$$\sigma_{\alpha,i} = -s_\alpha \operatorname{sgn}(V_\alpha)\langle\hat{O}_\alpha\rangle_{\sigma=0} \tag{6.6}$$

for a starting configuration also leads to a shorter thermalization time than the choice of $\sigma = 0$.

B. Examples

We now describe several examples to demonstrate our methods for calculating nuclear properties. Two major considerations arise in the implementation: the choice of decomposition scheme and the choice of ensemble. Different decomposition schemes involve different dimensions of matrices and numbers of fields, which control the computational speed. Also, the rates of convergence as $\Delta\beta \to 0$ are different and determine the number of time slices to be used. Finally, and perhaps most importantly, this choice also affects the "sign problem" associated with the statistical stability of the calculation. Different decomposition schemes will be compared in examples 1 and 2 below.

The choice of ensemble among zero-temperature, canonical, and grand-canonical ensembles usually does not affect the issues noted above. Instead, it depends on the kind of properties to be calculated. The zero-temperature formalism with a good trial wave function

is effective in projecting out the ground state and is suitable for calculating ground-state static observables. For calculating finite-temperature properties, the canonical ensemble is physically most relevant but also is most difficult to implement. Examples 1, 2, and 3 below demonstrate the grand-canonical, zero-temperature, and canonical ensembles, respectively.

Finally, we choose a particular nucleus, ^{20}Ne, to demonstrate the calculation of the dynamical responses for different operators and recover the strength function by the ME method. The examples shown below were done with 3000–6000 samples generated on the passively parallel Touchstone Gamma and Delta computers at Caltech.

1. Example 1:
Monopole pairing interaction in the sd shell

We have described the considerable flexibility in writing the two-body interaction in quadratic form, e.g., density versus pairing decomposition and direct versus exchange decomposition. To illustrate this flexibility, we consider protons only in the sd shell ($N_s = 12$), and keep only the $J = 0$ terms in Eq. (3.5); the values of $V_{J=0}$ and single-particle energies are taken from the Wildenthal interaction [1]. We first recouple the Hamiltonian into a quadratic form in the density operators in Eq. (3.21); because all possible density operators are required, there are 144 fields for each time slice. We then use the pairing decomposition in Eq. (3.41); after diagonalization only 6 fields are required. Finally, we write the two-body interaction as $\hat{H}_2 = \frac{1}{2}\hat{H}_2 + \frac{1}{2}\hat{H}_2$ and decompose the first half using densities and the second half using pairs; the total number of fields in this case is 150. It turns out that this system is 99% free of the sign problem [i.e., $\mathrm{Re}(\Phi_i) > 0$ 99% of the time], independent of the decomposition.

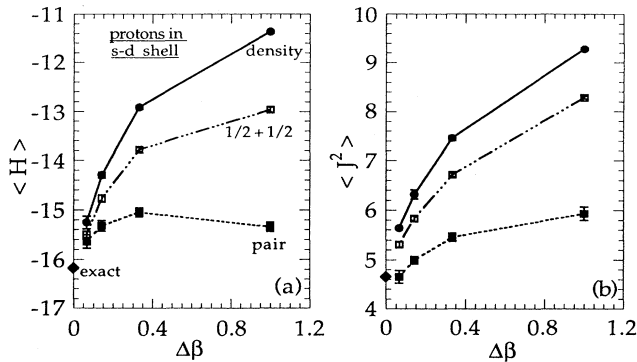All three calculations were performed in the grand-

FIG. 1. Calculations in the grand-canonical ensemble for protons only in the sd shell with monopole interaction (all six $E_{J=0}$ matrix elements of the Wildenthal interaction), at $\langle N_p \rangle = 3.17$, $\beta = 1$. Shown are $\langle H \rangle$ and $\langle J^2 \rangle$ as functions of $\Delta\beta$ for three different decompositions: pure pairing decomposition; pure density decomposition, and a half-density and half-pairing decomposition. Solid diamonds at $\Delta\beta = 0$ are the exact results obtained by direct diagonalization.

canonical ensemble using a Gaussian weight function around the static mean field, at an inverse temperature of $\beta = 1$ (here, and henceforth, we measure all physical energies in MeV) and fixed chemical potential. The expectation value of the proton number, energy, and J^2 are given in Fig. 1 as a function of $\Delta\beta$. As the number of time slices increases (i.e., $\Delta\beta \to 0$), all three decompositions converge to the exact answer, demonstrating their mutual equivalence in the continuum limit. Note, however, the different rates of convergence.

2. Example 2: ^{24}Mg with schematic forces

Next we consider sd-shell nuclei with a schematic pairing + multipole density interaction, where the multipole force is separable; it is the same interaction used in [7]:

$$\hat{H}_2 = -g \sum_{T_z=-1,0,1} P_{T_z}^\dagger P_{T_z} - \frac{1}{2}\chi_0 \bar{\rho}_{0,0}\bar{\rho}_{0,0}$$
$$- \frac{1}{2}\chi_2 \sum_M \bar{\rho}_{2,M}\bar{\rho}_{2,-M}(-1)^M$$
$$- \frac{1}{2}\chi_4 \sum_M \bar{\rho}_{4,M}\bar{\rho}_{4,-M}(-1)^M , \qquad (6.7)$$

where

$$P_{T_z} = \sum_{jmt_1t_2} (\tfrac{1}{2}t_1 \tfrac{1}{2}t_2 | 1T_z) a_{jmt_1}\tilde{a}_{jmt_2} \qquad (6.8)$$

and

$$\bar{\rho}_{K,M} = \sum \tilde{u}_K(j_1 j_2)\rho_{K,M,T=0}(j_1,j_2) . \qquad (6.9)$$

This Hamiltonian was also decomposed in several ways. We first decomposed the pairing interaction as pair operators and the multipole force as density operators. In this way, the number of fields is kept to a minimum (only 21 per time slice). The pair operator $P_{T_z=0}$ mixes protons and neutrons and therefore one matrix representing the mixed neutron and proton wave function is needed. In addition, the pairing decomposition requires matrices whose dimension is $2N_s$, so that the matrices involved in this calculation are 48 × 48.

We calculated ^{24}Mg (four valence protons and four valence neutrons) in the zero-temperature formalism, i.e., using the evolution operator at large β to project out the ground state from a trial state ψ_0. Since $\hat{h}$ is Hermitian [here $\bar{\rho}$ has the property $\bar{\rho}_{K,M}^\dagger = \bar{\rho}_{K,-M}(-1)^M$], in the static path $\zeta = \langle \psi_0 | \exp(-\beta\hat{h}) | \psi_0 \rangle$ is always positive definite and $\Phi_i = 1$. However, for calculations with more than one time slice $\langle \Phi \rangle$ becomes very small, so that we can only obtain sensible results in the SPA. These results turned out to be extremely good, relaxing to the right energy and angular momentum (Fig. 2). However, the success of the static path is case specific and not well understood. For example, we have also tried the case of just multipole interactions among four protons in the sd

shell (^{20}Mg), and find that the SPA relaxes to an energy 2 MeV higher than the ground state.

In a second scheme, we transformed the pairing part of the interaction (6.7) into a quadratic form in the density operators. In this transformation, we used only density operators that conserve proton and neutron numbers (3.24–3.34), and chose all $E_{K,T=1}$ elements in Eq. (3.27) to be zero so that only isoscalar density operators were present in the quadratic form.

In this case, the interaction is in a much more complicated form due to the Pandya transformation of the pairing interaction, and one needs 144 fields per time slice (as compared to 21 fields needed in the first decomposition). However, an advantage lies in the separation of the Slater determinants for protons and neutrons since only density operators that separately conserve neutron and proton numbers are present. In the sd shell, the dimension of matrix involved is only 12×12. For this particular interaction, an even more desirable property of the second scheme is that the eigenvalues $\lambda_{K,\alpha}$ in Eq. (3.34) found by diagonalizing E_K in Eq. (3.27) satisfy $\text{sign}(\lambda_K) = (-1)^{K+1}$. We prove in the next section that this property guarantees $\zeta(\sigma)$ to be positive definite for even-even nuclei if a suitable trial state is chosen. This allows calculations with any number of time slices that are free from any sign problem.

We performed the calculation using the zero-temperature formalism at different β and $\Delta\beta$ values, choosing first the Hartree Slater determinant as the trial wave function. The SPA calculation and that with $\Delta\beta = 0.125$ are shown in Fig. 2. We have also performed calculations at $\Delta\beta = 0.5$ and $\Delta\beta = 0.25$. These results are not shown but lie between the SPA and the $\Delta\beta = 0.125$ results, and show a convergence to the re-

sult at $\Delta\beta = 0.125$. At $\Delta\beta = 0.125$, the energy relaxes to the right energy, whereas the SPA also relaxes, but to a much higher energy.

We repeated these last calculations with a different trial wave function: a Slater determinant of the orbitals $(j, m) = (\frac{5}{2}, \pm\frac{1}{2}), (\frac{5}{2}, \pm\frac{3}{2})$. Although a different relaxation curve is traced out by the results at $\Delta\beta = 0.125$, it also converges to the same exact result (Fig. 2). The choice of the trial state is therefore important for determining the rate of relaxation of the zero-temperature approach, although the final result is independent of the trial state as expected. In this case, although the Hartree state is lower in energy than the maximal prolate state (compare $\langle H \rangle$ at $\beta = 0$), it contains some high angular momentum components (compare $\langle J^2 \rangle$ at $\beta = 0$), so that it relaxes more slowly and reaches the ground state at a larger value of β.

3. Example 3:
Canonical calculations of ^{20}Ne and ^{24}Mg

Next, we demonstrate the canonical ensemble for the same interaction (6.7) using the pure density decomposition as described in example 2. We calculate ^{20}Ne because it is small enough to allow for an exact diagonalization to give all the states of $\hat{H}$, since we are concerned with both ground-state and thermal properties. The canonical trace for this path integral in also positive definite (see Sec. VII), allowing the calculations to be done using many time slices.

The results for calculations with $\Delta\beta = 0.25, 0.125$, and 0.0625 are shown in Fig. 3. The convergence as a function of $\Delta\beta$ is also apparent. Note that particular attention should be given to the extrapolation at high temperature. However, it is not hard to increase the number of time slices to decrease the error at high temperature. For example, for $\beta = 0.5, \Delta\beta = 0.0625$ amounts to only eight time slices. Similar results on ^{24}Mg in the canonical ensemble are shown in Fig. 4. The relaxation to the ground
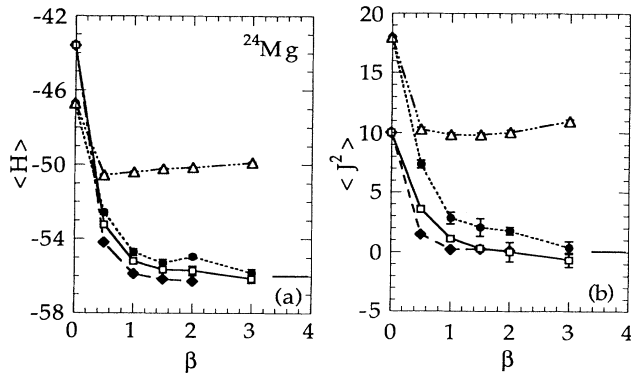

FIG. 2. Zero-temperature calculations of ^{24}Mg with the schematic interaction (6.7). Note the relaxation of $\langle H \rangle$ and $\langle J^2 \rangle$ as β increases. Hollow triangles are static path calculations in the pure density decomposition; solid diamonds are static path calculations by decomposing the pairing interaction into pair operators and the multipole interaction into density operators. Solid circles and hollow squares are both calculations in a pure density decomposition with $\Delta\beta = 0.125$, using the Hartree solution and the maximal prolate state, respectively, as the trial wave function. The solid line segments indicate the exact ground-state results.
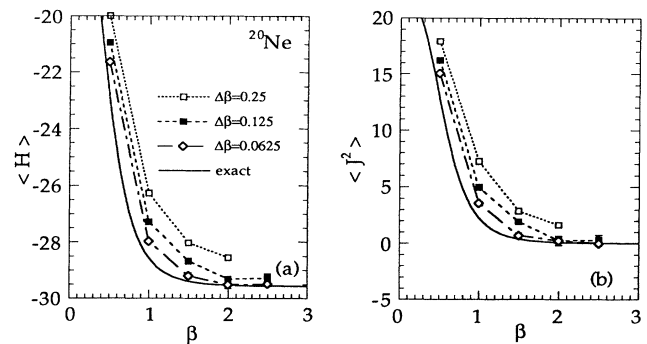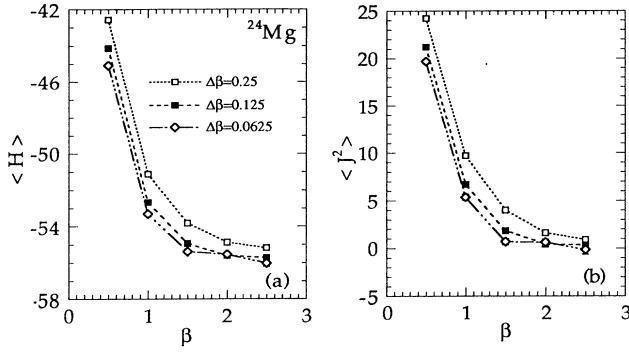

FIG. 3. Canonical ensemble calculations of ^{20}Ne with the schematic interaction (6.7) at $\Delta\beta = 0.25, 0.125$, and 0.0625 and the exact results; $\langle H \rangle$ and $\langle J^2 \rangle$ are shown as functions of β. These calculations were done in a pure density decomposition.

FIG. 4. Similar to Fig. 3 for ^{24}Mg.

state can be compared with the zero-temperature result in Fig. 2; however, now the results at small values of β are also physically significant.

In the calculation of ^{20}Ne, the activity expansion method is numerically stable. However, instabilities appear for sd nuclei when the number of proton or neutron valence particles (or holes) is greater than 4. The instability is signaled by the deviation of $\langle N_p \rangle$ and $\langle N_n \rangle$ from integers. In those cases, the expansion in Eq. (4.27) or (4.35) gives the canonical trace as the small difference between very large numbers, so that midshell nuclei cannot be calculated directly by those equations. We have developed an alternative Fourier expansion technique to extract the canonical trace that gives satisfactory results [12].

The real coherent-state method for the canonical trace for ^{24}Mg gives the same results as the activity expansion. However, $\langle \Phi_i \rangle$ is not always unity due to the need to integrate over the coherent states in Eq. (4.40) (as will be explained in the next section). It changes from 0.70 to 0.23 for β changing from 0.5 to 1.0 at $\Delta\beta = 0.25$.

We have also studied rotating nuclei in the canonical ensemble by adding a Lagrange multiplier to the Hamiltonian, $\hat{H}' = \hat{H} - \omega \hat{J}_z$, where $\hat{J}_z$ is the z component of the angular momentum and ω is the cranking frequency. The calculations at $\beta = 1$ for ^{20}Ne with $\Delta\beta = 0.125, 0.0625$, and 0.03125 are shown in Fig. 5, where the convergence

to the exact results can be seen. The moments of inertia fitted from the three sets of data are 5.10, 5.30, and 4.95, compared to 4.74, the value from the exact curve. By adding the term linear in $\hat{J}_z$, we break the time-reversal symmetry of $\hat{h}(\sigma)$, which is related to the sign properties of the weight function $\zeta(\sigma)$. $\langle \Phi \rangle$ decreases from 1 to 0.55 when ω is increased from 0 to 1.5 at $\Delta\beta = 0.125$ while it decreases from 1 to 0.52 at $\Delta\beta = 0.03125$.

4. Example 4:
Response and strength functions for ^{20}Ne

Finally, we demonstrate calculation of the imaginary-time response functions and the reconstruction of the strength functions. The calculation for ^{20}Ne is done by the activity expansion method in a pure density decomposition; the Hamiltonian is that of Eq. (6.7). The canonical ensemble is more suitable than the zero-temperature formalism for measuring the dynamical response, because in the latter case many "boundary" time slices are needed to project out the ground state on both the left and the right, and extra time slices would have to be introduced in the middle to measure the response. In contrast, the cyclic property of the trace allows full use to be made of every time slice in the canonical ensemble. We choose $\beta = 2.5$ (the system has already reached the ground state at this low temperature, as can be seen from Fig. 3) and calculate the response functions at $\Delta\beta = 0.125$ and $\Delta\beta = 0.0625$ for several one-body operators: the isovector- and the isoscalar-quadrupole operators $\hat{Q}_v = \hat{Q}_p - \hat{Q}_n$, $\hat{Q}_s = \hat{Q}_p + \hat{Q}_n$, and the isoscalar and isovector angular momentum operators $\hat{J}_s = \hat{J}_p + \hat{J}_n$, $\hat{J}_v = \hat{J}_p - \hat{J}_n$. We choose this latter 1^+ operator purely out of convenience; $\hat{J}_s$ is just the total angular momentum, which we verified to produce a constant response equal to $\langle \hat{J}^2 \rangle$, which follows from the rotational invariance of $\hat{H}$.

The response functions are shown in a semilog plot in Figs. 6(a,c,e). For these Hermitian operators, $R(\tau)$ is symmetric about $\tau = \beta/2$, and so it is shown only for $\tau \le \beta/2$. The slope of the plot is approximately the energy of the dominant strength. The $\hat{J}_v$ and $\hat{Q}_v$ responses relax more rapidly than does the $\hat{Q}_s$ response, indicating that
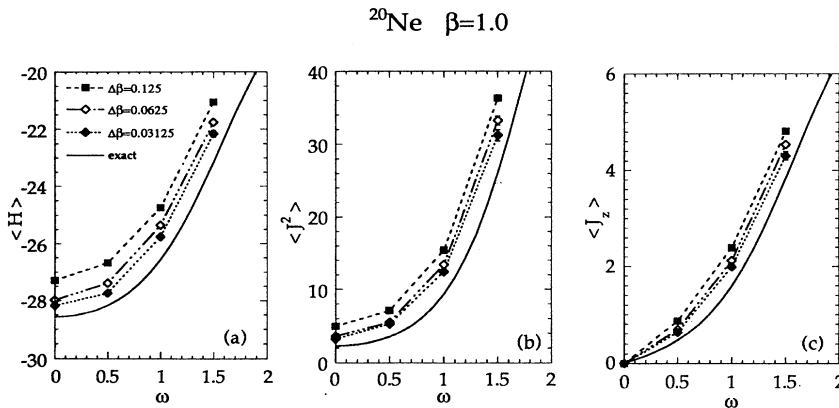
^{20}Ne $\beta = 1.0$

FIG. 5. Finite-temperature cranked calculations of ^{20}Ne with the schematic interaction (6.7) in the canonical ensemble using a pure density decomposition. Here $\beta = 1$, with $\Delta\beta = 0.125, 0.0625$, and 0.03125. The exact cranking curve is also shown.

TABLE I. ME extraction of the moments of the strength functions corresponding to Figs. 6 and 7. The extrapolated ($\Delta\beta \to 0$) total strength and first two moments are compared with the exact results for the ground state of ^{20}Ne.

		$\Delta\beta = 0.125$	$\Delta\beta = 0.0625$	extrap.	exact
$Q(\tau) \cdot Q(0)$	total strength	27.3 ± 0.2	25.9 ± 0.1	24.5	25.1
	$\langle\omega\rangle$	2.33 ± 0.08	2.77 ± 0.08	3.22	3.46
	$\langle\omega^2\rangle$	8.09 ± 1.2	10.5 ± 1.2	12.9	15.4
$Q_v(\tau) \cdot Q_v(0)$	total strength	6.26 ± 0.03	6.78 ± 0.02	7.29	6.96
	$\langle\omega\rangle$	7.24 ± 0.15	7.77 ± 0.10	8.31	8.38
	$\langle\omega^2\rangle$	59.9 ± 3.9	66.6 ± 2.5	73.4	73.8
$J_v(\tau) \cdot J_v(0)$	total strength	16.3 ± 0.1	16.05 ± 0.08	15.8	15.9
	$\langle\omega\rangle$	8.49 ± 0.25	9.44 ± 0.19	10.39	10.39
	$\langle\omega^2\rangle$	89.8 ± 9.04	107.7 ± 6.4	125.6	119.6
$\sum_m a^\dagger_{5/2m}(\tau)a_{5/2m}(0)$	total strength	1.59 ± 0.01	1.62 ± 0.07	1.64	1.59
	$\langle\omega\rangle$	9.84 ± 0.12	10.32 ± 0.09	10.80	10.98
	$\langle\omega^2\rangle$	98.0 ± 2	107.5 ± 1.4	117	121
$\sum_m a_{5/2m}(\tau)a^\dagger_{5/2m}(0)$	total strength	4.47 ± 0.01	4.42 ± 0.09	4.37	4.41
	$\langle\omega\rangle$	-3.15 ± 0.02	-3.00 ± 0.02	-2.86	-2.81
	$\langle\omega^2\rangle$	10.28 ± 0.05	9.71 ± 0.04	9.14	10.08
$\sum_m a_{1/2m}(\tau)a^\dagger_{1/2m}(0)$	total strength	1.702 ± 0.004	1.745 ± 0.003	1.788	1.773
	$\langle\omega\rangle$	-3.19 ± 0.01	-3.22 ± 0.02	-3.25	-3.16
	$\langle\omega^2\rangle$	10.43 ± 0.06	10.65 ± 0.04	10.87	11.62

the two isovector operators couple to states with higher excitation energy than does the $\hat{Q}_s$ operator. Since ^{20}Ne has a $J = 0$, $T = 0$ ground state, the states excited by an operator will carry the J and T quantum numbers of the operator. The plots are therefore consistent with the existence of a low-lying 2^+ state.

The ME reconstructions of the most probable strength function for the different one-body operators are shown in Figs. 6(b,d,e). The reconstruction is performed for each response function measured at each $\Delta\beta$ value. The figures show the convergence in $\Delta\beta$ of the resulting strength functions to the exact strength function. Note the move-
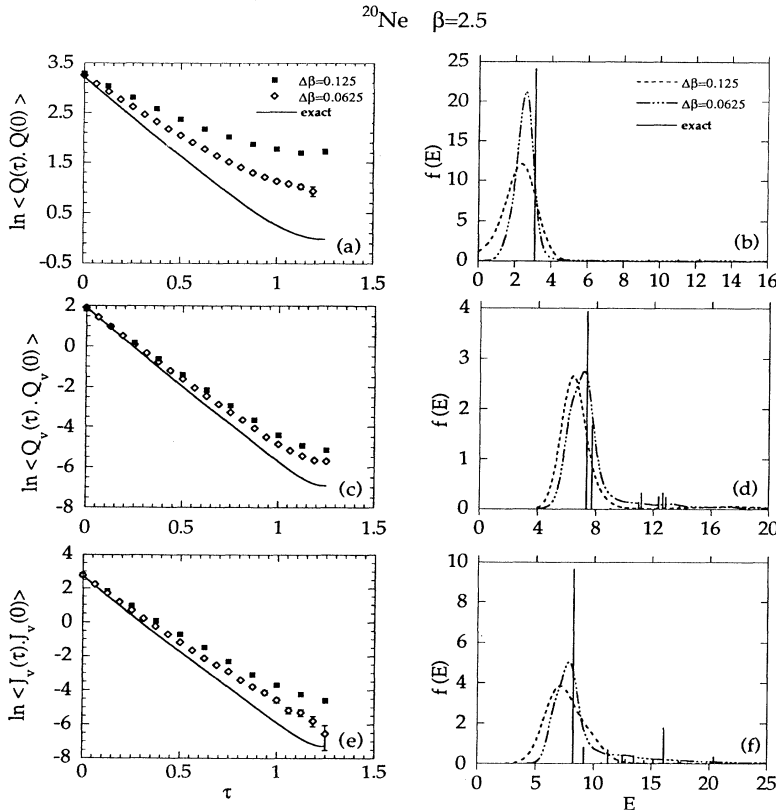

^{20}Ne β=2.5

FIG. 6. Canonical ensemble calculations of the response functions for ^{20}Ne ($\beta = 2.5$) at discrete imaginary time using $\Delta\beta = 0.125, 0.0625$, in a pure density decomposition. The exact results are calculated in the ground state. (a), (c), (e) The isoscalar quadrupole ($Q = Q_p + Q_n$), isovector quadrupole ($Q_v = Q_p - Q_n$), and the isovector angular angular momentum ($J_v = J_p - J_n$) responses. The corresponding most probable strength functions recovered by the ME method are shown in (b), (d), (f), respectively. The exact strength functions calculated from ground state are plotted as discrete lines with the height indicating the integrated strength of the delta functions.
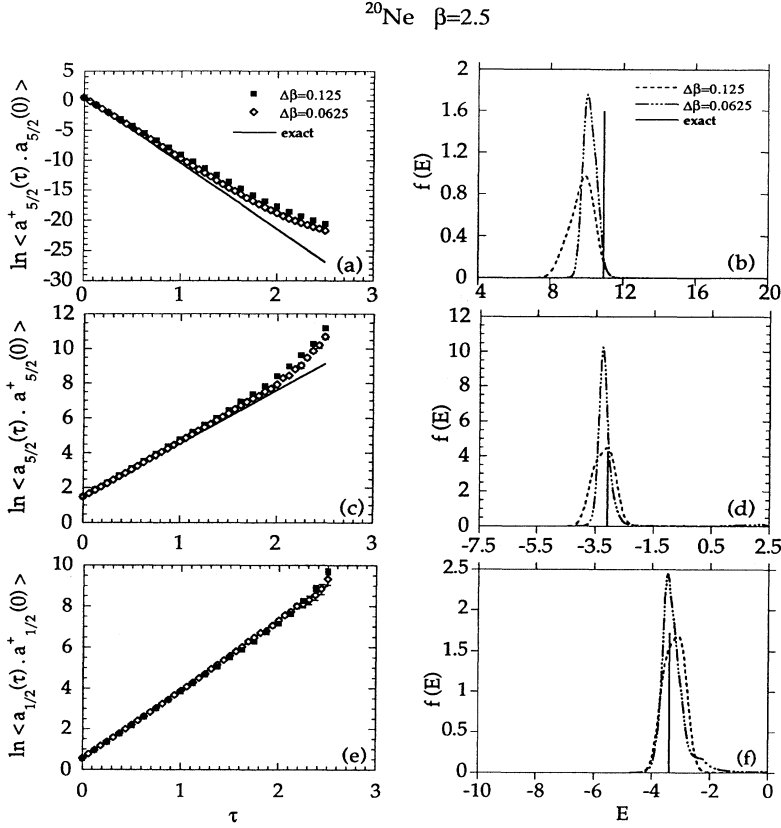
FIG. 7. Similar to Fig. 6 but for the single-particle pickup and stripping response. (a), (c), (e) The imaginary time stripping response for the $j = \frac{5}{2}$ orbital and the pickup responses of the $j = \frac{5}{2}$ and $j = \frac{1}{2}$ orbitals, respectively. The corresponding most probable strength functions recovered by the ME method are shown in (b), (d), (f), respectively. The exact response and strength functions are calculated for the ground state.

ment of the peaks towards the exact position and also the decrease in the widths as $\Delta\beta$ decreases.

The average nth moments of the strength function, defined by

$$M_n \equiv \sum_i \omega_i^n f(\omega_i) , \qquad (6.10)$$

can be found in the Monte Carlo integration over all the possible distributions of the f_i. Their uncertainties can be determined similarly. The first moment $\langle M_1 \rangle$ and the second moment $\langle M_2 \rangle$ of the strength functions are listed in Table I for different operators and different $\Delta\beta$. The extrapolated moments ($\Delta\beta \to 0$) and the exact results for the ground-state transitions are also shown.

The single-particle pickup and stripping response functions for different orbitals are given in a semilog plot in Figs. 7(a,c,e) and Fig. 8. The strength functions extracted from these responses are related to the excitation spectrum in the neighboring nucleus with one additional particle or hole. The stripping and pickup responses are the same for protons and neutrons as the ground state of ^{20}Ne is isoscalar, and the final states have the angular momentum of the single nucleon that is added or removed. We see from Fig. 7 that both the pickup and stripping responses for the $j = \frac{5}{2}$ orbital and the pickup response for the $j = \frac{1}{2}$ orbital converge to the exact results as $\Delta\beta$ becomes small; the ME reconstruction of the corresponding strength functions in Figs. 7(b,d,e) also show a convergence to the exact results. The extracted

moments are listed in Table I. However, the responses for the $j = \frac{3}{2}$ orbital show an anomalous behavior: They are close to the exact result at $\tau = 0$, and then, with a sudden change in slope, follow the responses of the $j = \frac{5}{2}$ orbital. A possible reason is that angular momentum is not conserved sample by sample in the calculation, but rather only statistically. The $J = \frac{5}{2}$ states for ^{19}Ne and ^{20}Ne nuclei are much lower in energy than the $J = \frac{3}{2}$ states (because the $j = \frac{5}{2}$ orbital is lower than the $j = \frac{3}{2}$
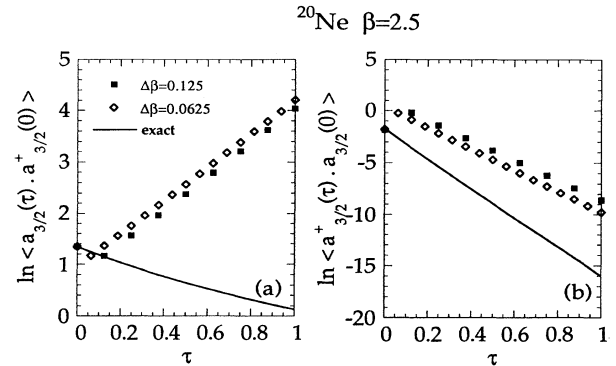

FIG. 8. Similar to Figs. 6, 7 but showing the imaginary time pickup and stripping responses of $j = \frac{3}{2}$ orbital. The response functions are in agreement with the exact curve for small τ, but then abruptly follow the $j = \frac{5}{2}$ response at larger τ.

orbital by 5.6 MeV), so that if a small admixture of the $J = \frac{5}{2}$ states "leaks" into the intermediate states for the $j = \frac{3}{2}$ response, it will dominate with an exponentially growing correlation function. (The $j = \frac{1}{2}$ orbital is much closer to the $j = \frac{5}{2}$ orbital in comparison, only 0.8 MeV higher.)

VII. SIGN PROBLEM AND FUTURE DEVELOPMENTS

We have seen in the examples above that the sign properties for the function $G(\sigma)\zeta(\sigma)$ are crucial to the stability of the calculation, and may frustrate attempts to apply the Monte Carlo path integral to any general two-body interaction. In general, if we choose an arbitrary two-body interaction and arbitrarily decompose it into pair or density operators, $\langle\Phi\rangle$ vanishes rapidly as β increases or as the number of time slices N_t increases at a fixed β. For example, with the Wildenthal interaction and for any calculation for $\beta > 1$ with more than three time slices, the noise due to the sign completely swamps the signal. This "sign problem" is well known in auxiliary-field path-integral calculations [20] and fermion quantum Monte Carlo more generally. If there is no explicit symmetry to enforce the positivity of ζ_σ, $\langle\Phi\rangle$ decays exponentially as a function of β, and the problem is more severe for smaller $\Delta\beta$, so that it is very difficult to calculate low-temperature properties.

Only a handful of interacting fermion systems are known to give rise to a positive-definite path integral: the one-dimensional Hubbard model, the half-filled Hubbard model, and the attractive Hubbard model at any dimension and filling [3]. We will show in the following that an important class of interactions for the nuclear shell model has a positive-definite path-integral representation for even-even nuclei. It arises from the symmetry between time-reversed single-particle orbitals and may serve as a starting point in understanding and controlling the "sign problem."

We first define the "time-reversed" partner of each creation and annihilation operator to be

$$\tilde{a}_{j,m} \equiv a_{j,\bar{m}} = (-1)^{j+m} a_{j,-m} \ , \qquad (7.1\text{a})$$

$$\tilde{a}^\dagger_{j,m} \equiv a^\dagger_{j,\bar{m}} = (-1)^{j+m} a^\dagger_{j,-m} \ . \qquad (7.1\text{b})$$

Note that

$$\tilde{\tilde{a}}_{j,m} = -a_{j,m} \qquad (7.2)$$

due to the spin-half statistics.

The class of Hamiltonians that give rise to a positive-definite path integral are of the form

$$\hat{H} = -\frac{1}{2}\sum_\alpha \chi_\alpha \rho_\alpha \tilde{\rho}_\alpha + e_\alpha \rho_\alpha + e^*_\alpha \tilde{\rho}_\alpha \ , \qquad (7.3)$$

where $\chi_\alpha > 0$, e_α can be generally complex, and ρ_α is a general density operator of the form

$$\rho_\alpha = \sum_{ij} C_{ij} a^\dagger_i a_j \ . \qquad (7.4)$$

Note the requirement of a negative coupling constant for the density operator with its time-reversed partner and the time-reversal invariant form of the remaining one-body part.

For application to the shell model, we refer to Eq. (3.17), so that, in the density decomposition,

$$\tilde{\rho}_{KM}(\alpha) = (-1)^{K+M}\rho_{K-M}(\alpha) \ . \qquad (7.5)$$

The requirement of a negative coupling constant for the density operators leads to a sign rule for the $\lambda_{K\alpha}$, namely,

$$\text{sgn}(\lambda_{K\alpha}) = (-1)^{K+1} \ . \qquad (7.6)$$

As we will show below, the Hamiltonian (7.3) gives rise to a one-body Hamiltonian in the path integral, $\hat{h}_\sigma$, that is symmetric in time-reversed orbitals. Time-reversed pairs of single-particle orbitals thus acquire complex-conjugate phases in the propagation, guaranteeing a positive-definite overlap function ζ.

After the HS transformation on Eq. (7.3), the linearized Hamiltonian is

$$\hat{h} = -\sum_\alpha \chi_\alpha[(\sigma_\alpha + i\tau_\alpha)\rho_\alpha + (\sigma_\alpha - i\tau_\alpha)\tilde{\rho}_\alpha]$$
$$+e_\alpha \rho_\alpha + e^*_\alpha \tilde{\rho}_\alpha \ , \qquad (7.7)$$

so that ρ and $\tilde{\rho}$ couple to complex-conjugate fields. [If some part of the interaction does not satisfy (7.6), then there will be terms in $\hat{h}$ that are of the form $i(\sigma_\alpha + i\tau_\alpha)\rho_\alpha + i(\sigma_\alpha - i\tau_\alpha)\tilde{\rho}_\alpha$, and the above statement is not true.]

We represent the single-particle wave function by a vector of the form

$$\begin{pmatrix} jm \\ j\bar{m} \end{pmatrix}, \quad m > 0 \ , \qquad (7.8)$$

with states with $m > 0$ in the first half of the vector and their time-reversed orbitals in the second half. Due to Eq. (7.3) and the fact that time-reversed operators are coupled to complex-conjugate fields, the matrix $\mathbf{M}_i$ representing $\hat{h}_i$ has the structure

$$\mathbf{M}_i = \begin{pmatrix} \mathbf{A}_i & \mathbf{B}_i \\ -\mathbf{B}^*_i & \mathbf{A}^*_i \end{pmatrix} \ , \qquad (7.9)$$

and one can easily verify that the total evolution matrix

$$\mathbf{U} = \prod_i \exp(-\mathbf{M}_i\Delta\beta) = \begin{pmatrix} \mathbf{P} & \mathbf{Q} \\ -\mathbf{Q}^* & \mathbf{P}^* \end{pmatrix} \qquad (7.10)$$

is of the same form. Here, $\mathbf{A}$, $\mathbf{B}$, $\mathbf{P}$, $\mathbf{Q}$ are matrices of dimension $N_s/2$. One can show that this matrix has pairs of complex-conjugate eigenvalues ϵ, ϵ^* with respective eigenvectors $\begin{pmatrix} u \\ v \end{pmatrix}$ and $\begin{pmatrix} -v^* \\ u^* \end{pmatrix}$. In the case where ϵ is real, it is doubly degenerate since the two eigenvectors are distinct.

For the grand-canonical ensemble, the overlap function is given by

$$\zeta = \det\left[1 + \begin{pmatrix} \mathbf{P} & \mathbf{Q} \\ \mathbf{Q}^* & \mathbf{P}^* \end{pmatrix}\right] = \prod_i^{N_s/2} (1 + \epsilon_i)(1 + \epsilon_i^*) > 0 \ .$$

$$(7.11)$$

If only particle-type (neutron-proton) conserving density operators are present in Eq. (7.3), each type of nucleon is represented by a separate Slater determinant having the structure (7.10), and therefore $\zeta = \zeta_p \times \zeta_n > 0$, since $\zeta_p > 0$ and $\zeta_n > 0$.

In the zero-temperature formalism, if the trial wave function for an even number of particles is chosen to consist of time-reversed pairs of single-particle states,

$$\boldsymbol{\Psi}_0 = \begin{pmatrix} \mathbf{a} & \mathbf{b} \\ -\mathbf{b}^* & \mathbf{a}^* \end{pmatrix} \ , \qquad (7.12)$$

where $\mathbf{a}, \mathbf{b}$ are matrices with dimension $(\frac{N_s}{2} \times \frac{N_v}{2})$, then $\boldsymbol{\Psi}_0^\dagger \mathbf{U} \boldsymbol{\Psi}_0$ is a $N_v \times N_v$ matrix with the structure (7.10), and the overlap function again satisfies

$$\zeta = \det[\boldsymbol{\Psi}_0^\dagger \mathbf{U} \boldsymbol{\Psi}_0] > 0 \ . \qquad (7.13)$$

If only particle-type conserving operators are present, then time-reversed pairs of trial wave functions can be chosen for both protons and neutrons in an even-even nucleus, giving rise to $\zeta = \zeta_p \times \zeta_n > 0$. Note that while the overlap function is positive definite in the grand-canonical ensemble for any chemical potential (and thus any average number of particles), it is true only for an even (or even-even if involving a type-conserving decomposition) system in the zero-temperature formalism with a suitable trial wave function.

In the canonical ensemble for N particles, a fixed-number trace is involved and therefore

$$\zeta\left(\prod_i \exp(-\mathbf{M}_i \Delta\beta)\right) = \sum_{i1 \neq i2 \neq \dots i_N} \epsilon_{i1} \epsilon_{i2} \dots \epsilon_{i_N} \ .$$

$$(7.14)$$

We have found empirically that ζ is positive definite for even-even systems, although we lack a rigorous proof. A special case of the Hamiltonian (7.2) exists in which the overlap function is positive definite also for odd-odd $N = Z$ nuclei. The required condition is that only isoscalar density operators are present in Eq. (7.2). This leads to a further symmetry that protons and neutrons couple to the same field in Eq. (7.7) and therefore the evolution matrices satisfy $\mathbf{U}_p = \mathbf{U}_n \equiv \mathbf{U}$. In the zero-temperature formalism, if we choose the trial wave function for proton and neutrons to be time-reversed partners of each other, so that

$$\boldsymbol{\Psi}_{0,p} = \begin{pmatrix} \mathbf{a} \\ \mathbf{b} \end{pmatrix}, \quad \boldsymbol{\Psi}_{0,n} = \begin{pmatrix} -\mathbf{b}^* \\ \mathbf{a}^* \end{pmatrix} \ , \qquad (7.15)$$

and then

$$\begin{aligned} \zeta_p &= \det[\boldsymbol{\Psi}_{0,p}^\dagger \mathbf{U} \boldsymbol{\Psi}_{0,p}] \\ &= \det[\mathbf{a}^\dagger \mathbf{P} \, \mathbf{a} + \mathbf{a}^\dagger \mathbf{Q} \, \mathbf{b} - \mathbf{b}^\dagger \mathbf{Q}^* \mathbf{a} + \mathbf{b}^\dagger \mathbf{P}^* \mathbf{b}] = \zeta_n^* \ , \end{aligned}$$

$$(7.16)$$

and $\zeta = \zeta_p \times \zeta_n > 0$. On the other hand, for the canonical ensemble, one can prove that Eq. (7.13) is real. Given that $\zeta_n = \zeta_p$, ζ is a square and is therefore positive.

For a system with general form (7.3), if we perform the canonical trace by integration over real coherent states, then there is an extra operator, $\exp(X_{ph} a_p^\dagger a_h)$, multiplying the evolution operator. Time-reversed states couple to different real fields in the extra operator, and a sign problem arises, as seen in example 3 above.

Cranking also causes the sign to depart from unity. In cranking, the Lagrange multiplier term ωJ_z is added to $\hat{h}$ in Eq. (7.7), destroying the property that time-reversed operators are coupled to complex-conjugate numbers (because $\tilde{J}_z = -J_z$). Notice, however, that cranking with an imaginary Lagrange multiplier $i\omega J_z$ will preserve the time-reversal symmetry and will give rise to a positive path integral.

In summary, for a Hamiltonian of the form (7.3), the above proof guarantees the overlap function to be positive for any nucleus in the grand-canonical ensemble, and for even-even nuclei in either the canonical ensemble or zero-temperature formalism (with suitable trial wave function). It also guarantees positivity for odd-odd $N = Z$ systems when only isoscalar density operators are involved.

The Hamiltonian (6.7) satisfies (7.6) upon decomposition of the paring interaction using density operators and involves only isoscalar operators, so that ζ is positive for even-even and $N = Z$ nuclei. For other systems, $\langle \Phi \rangle$ decreases as a function of β. At $\Delta\beta = 0.0625$, $\langle \Phi \rangle = 0.4$ at $\beta = 1.5$ for ^{24}Na, and $\langle \Phi \rangle = 0.2$ at $\beta = 2.0$ for ^{23}Na. Thus, even for odd-A nuclei, the sign properties of (6.7) are still much better than that of a general interaction violating the criteria (7.6). For example, using the Wildenthal interaction, $\langle \Phi \rangle$ drops to several percent at $\beta = 1$ for any nucleus.

Arbitrary two-body interactions do not satisfy the sign rule (7.6), and when the rule is violated, $\langle \Phi \rangle$ rapidly decreases as a function of β. Note that monopole pairing plays an important role here. The pairing interaction can be written as

$$-g \sum_{ij} a_i^\dagger a_j \tilde{a}_i^\dagger \tilde{a}_j \ . \qquad (7.17)$$

It produces a constant shift in every χ_α in Eq. (7.3), as may be seen also from the multipole decomposition of the pairing force:

$$-g \sum_\alpha (-1)^K \rho_{KM}(\alpha) \rho_{K-M}(\alpha)(-1)^M \ . \qquad (7.18)$$

Therefore, if the pairing interaction is strong enough compared to the remaining interactions, the sign rule can be satisfied.

VIII. CONCLUSION

We have developed a general framework for carrying out auxiliary-field Monte Carlo calculations of the nu-

clear shell model. In this framework we evaluate ground-state or thermal observables, using pairing or density fields or both.

Although the use of pairing fields naturally embodies important aspects of the residual interaction, these calculations are more difficult due to the larger matrix dimension needed and the extra effort to keep track of the sign of the overlap function as the wave function is propagated. Furthermore, for calculations with multiple time slices, the Monte Carlo method with a pairing decomposition suffers from severe sign problems. However, pairing fields are suitable for carrying out static path or two-time-slice calculations where the linearized Hamiltonian is Hermitian, thereby enforcing the positivity of the overlap function. This can be easily verified by observing that for Hermitian $\hat{h}$, $\hat{h}_a$, and $\hat{h}_b$, with real eigenvalues E_i, E_{i_a}, and E_{i_b},

$$\hat{\text{Tr}}[e^{-\beta\hat{h}}] = \sum_i e^{-\beta E_i} > 0 \qquad (8.1)$$

and

$$\hat{\text{Tr}}[e^{-\frac{\beta}{2}\hat{h}_a}e^{-\frac{\beta}{2}\hat{h}_b}] = \sum_{i_a} e^{-\frac{\beta}{2}E_{i_a}} \langle i_a|e^{-\frac{\beta}{2}\hat{h}_b}|i_a\rangle > 0 . \qquad (8.2)$$

In these cases, there is no sign problem and also there is no need to keep track of the evolution of the sign.

For the density decomposition, we have found a class of interactions which give rise to a positive definite integrand upon the HS transformation. For these interactions, stable calculations can be carried out for many time slices to extrapolate to the exact results ($\Delta\beta \to 0$). This class of interactions includes the phenomenological pairing-plus-multipole interaction used widely. We have carried out calculations with such interactions in the sd shell, demonstrating the power of the method in calculating both static and dynamical properties in the ground state and at finite temperature; high spin nuclei were also studied by cranking. The calculations converge to the exact results (as found by direct diagonalization) with increasing number of time slices. Although the nuclear wave function is not found explicitly in these calculations, many nuclear properties can be obtained.

For general shell model interactions, it appears that the sign or phase property of the integrand is the major factor determining successful application of the Monte Carlo sampling. Successful calculations are usually confined to high-temperature studies. We have demonstrated the freedom one has in the decomposition scheme of the two-body interaction and found that the behavior of the sign can be different in the various schemes. The next crucial step is to explore whether we can manipulate these degrees of freedom to enable stable calculations of nuclei using general forces.

ACKNOWLEDGMENTS

APPENDIX A: DERIVATION OF THE OVERLAP FORMULAS FOR PAIRING FIELDS

We consider operators of the form

$$\hat{U} = \exp(-\Delta\beta\hat{h}_{N_t})\exp(-\Delta\beta\hat{h}_{N_t-1})\cdots\exp(-\Delta\beta\hat{h}_1) , \qquad (A1)$$

where each $\hat{h}_t$ is a quadratic operator,

$$\hat{h}_t = \sum_{i,j=1}^{Ns} \Theta(t)_{ij}a_i^{\dagger}a_j + \Delta(t)_{ij}a_i^{\dagger}a_j^{\dagger} + \Lambda(t)_{ij}a_ia_j . \qquad (A2)$$

Without loss of generality, we choose Δ, Λ to be antisymmetric ($\Delta = -\Delta^T$, etc.). We follow the development of Berezin [13], who considered the special case $\hat{U} = \exp(-i\hat{h}t)$ with $\hat{h}$ Hermitian; we take the general case.

We calculate the grand-canonical trace

$$\hat{\text{Tr}}\hat{U} = \sum_i \langle i|\hat{U}|i\rangle \qquad (A3)$$

(the sum is over all states of all particle number) by using the fermion coherent-state (FCS) representation of unity [21],

$$\mathbf{1} = \int \prod_\alpha d\xi_\alpha d\xi_\alpha^* \exp\left(-\sum_\alpha \xi_\alpha^*\xi_\alpha\right)|\xi\rangle\langle\xi|. \qquad (A4)$$

Here ξ_α are Grassman variables and the $|\xi\rangle$ are fermion coherent states. Then

$$\hat{\text{Tr}}\hat{U} = \int \prod_\alpha d\xi_\alpha d\xi_\alpha^* \exp\left(-\sum_\alpha \xi_\alpha^*\xi_\alpha\right)\langle\xi|\hat{U}|\xi\rangle. \qquad (A5)$$

We need the FCS representation of $\hat{U}$. In what immediately follows we show that if $\mathbf{U}$ is the matrix representation of $\hat{U}$, that is

$$\mathbf{U} \equiv \begin{pmatrix} \mathbf{U}^{11}\mathbf{U}^{12} \\ \mathbf{U}^{21}\mathbf{U}^{22} \end{pmatrix} \qquad (A6a)$$

$$\equiv \exp[-\mathbf{M}(N_t)\Delta\beta]$$
$$\times \exp[-\mathbf{M}(N_t-1)\Delta\beta]\cdots\exp[-\mathbf{M}(1)\Delta\beta] , \qquad (A6b)$$

where

$$\mathbf{M}(t) \equiv \begin{pmatrix} \Theta(t) & 2\Delta(t) \\ 2\Lambda(t) & -\Theta^T(t) \end{pmatrix} , \qquad (A7)$$

then

$$\langle\xi|\hat{U}|\xi\rangle = C \exp\left[\frac{1}{2}(\xi \quad \xi^*)\begin{pmatrix}\mathbf{B}^{11} & \mathbf{B}^{12}\\ \mathbf{B}^{21} & \mathbf{B}^{22}\end{pmatrix}\begin{pmatrix}\xi\\ \xi^*\end{pmatrix}\right],$$

$$\text{(A8)}$$

with

$$\mathbf{B}^{11} = \mathbf{U}^{22^{-1}}\mathbf{U}^{21}, \quad \mathbf{B}^{12} = -\mathbf{U}^{22^{-1}}, \quad \text{(A9a)}$$

$$\mathbf{B}^{21} = (\mathbf{U}^{22^{-1}})^T, \quad \mathbf{B}^{22} = \mathbf{U}^{12}\mathbf{U}^{22^{-1}}, \quad \text{(A9b)}$$

and

$$C = \det(\mathbf{U}^{22})^{\frac{1}{2}}\exp\left(-\frac{\Delta\beta}{2}\sum_{n=1}^{N_t}\text{Tr}\Theta(n)\right). \quad \text{(A10)}$$

In this case the trace becomes a Gaussian integral over Grassman variables; the result is given beginning with Eq. (A29) below. However, to come to that point we must derive Eqs. (A8)–(A10).

To this end, we employ the standard rules for operating on $|\xi\rangle, \langle\xi|$ with $a^\dagger, a$:

$$\langle\xi|\hat{U}\hat{a}_\alpha|\xi\rangle = \langle\xi|\hat{U}|\xi\rangle\xi_\alpha, \quad \text{(A11a)}$$

$$\langle\xi|\hat{U}a_\alpha^\dagger|\xi\rangle = \langle\xi|\hat{U}|\xi\rangle\frac{\overleftarrow{\partial}}{\partial\xi_\alpha}, \quad \text{(A11b)}$$

$$\langle\xi|a_\alpha^\dagger\hat{U}|\xi\rangle = \xi_\alpha^*\langle\xi|\hat{U}|\xi\rangle, \quad \text{(A11c)}$$

$$\langle\xi|a_\alpha\hat{U}|\xi\rangle = \frac{\partial}{\partial\xi_\alpha^*}\langle\xi|\hat{U}|\xi\rangle. \quad \text{(A11d)}$$

Next, we derive expressions for $a_\alpha\hat{U}, a_\alpha^\dagger\hat{U}$, as linear combinations of $\hat{U}a_\alpha, \hat{U}a_\alpha^\dagger$. Then, with the ansatz (A8) for $\langle\xi|\hat{U}|\xi\rangle$ as a Gaussian in the Grassman variables ξ, ξ^*, we use (A11) to derive the elements $\mathbf{B}$ of the Gaussian given in (A9).

To do this, we introduce the operators $b, \bar{b}$ (which are not necessarily Hermitian conjugates),

$$b_\alpha \equiv \hat{U}^{-1}a_\alpha\hat{U}, \quad \bar{b}_\alpha \equiv \hat{U}^{-1}a^\dagger\hat{U}. \quad \text{(A12a)}$$

Then

$$a_\alpha\hat{U} = \hat{U}b_\alpha, \quad a_\alpha^\dagger\hat{U} = \hat{U}\bar{b}_\alpha, \quad \text{(A12b)}$$

and we seek $b, \bar{b}$ as linear combinations of $a^\dagger, a$.

Define

$$a_\alpha(\tau) = e^{\hat{h}\tau}a_\alpha e^{-\hat{h}\tau}. \quad \text{(A13)}$$

Then

$$\frac{d}{d\tau}a_\alpha(\tau) = [\hat{h}, a_\alpha(\tau)], \quad \text{(A14)}$$

and similarly for $a_\alpha^\dagger(\tau)$. Putting all the $a_\alpha(\tau), a_\alpha^\dagger(\tau)$ into a single vector, and using the representation (A2) for $\hat{h}$, one finds

$$\frac{d}{d\tau}\begin{pmatrix}a(\tau)\\ a^\dagger(\tau)\end{pmatrix} = -\mathbf{M}\begin{pmatrix}a(\tau)\\ a^\dagger(\tau)\end{pmatrix}, \quad \text{(A15)}$$

with $\mathbf{M}$ given by (A7).

Solving the differential equation (A15),

$$\begin{pmatrix}a(\tau)\\ a^\dagger(\tau)\end{pmatrix} = \exp(-\mathbf{M}\tau)\begin{pmatrix}a\\ a^\dagger\end{pmatrix}, \quad \text{(A16)}$$

and so in general

$$\begin{pmatrix}b\\ \bar{b}\end{pmatrix} = \exp(\Delta\beta\hat{h}_1)\cdots\exp(\Delta\beta\hat{h}_{N_t})\begin{pmatrix}a\\ a^\dagger\end{pmatrix}$$
$$\times \exp(-\Delta\beta\hat{h}_{N_t})\cdots\exp(-\Delta\beta\hat{h}_1)$$
$$= \exp(-\Delta\beta\mathbf{M}_1)\cdots\exp(-\Delta\beta\mathbf{M}_{N_t})\begin{pmatrix}a\\ a^\dagger\end{pmatrix}$$
$$= \begin{pmatrix}\mathbf{U}^{11} & \mathbf{U}^{12}\\ \mathbf{U}^{21} & \mathbf{U}^{22}\end{pmatrix}\begin{pmatrix}a\\ a^\dagger\end{pmatrix}. \quad \text{(A17)}$$

Then

$$b_\alpha = \mathbf{U}^{11}{}_{\alpha\gamma}a_\gamma + \mathbf{U}^{12}{}_{\alpha\gamma}a_\gamma^\dagger, \quad \text{(A18a)}$$

$$\bar{b}_\alpha = \mathbf{U}^{21}{}_{\alpha\gamma}a_\gamma + \mathbf{U}^{22}{}_{\alpha\gamma}a_\gamma^\dagger, \quad \text{(A18b)}$$

where the summation on γ is implicit. Upon inserting (A18) in (A12b), and using the ansatz (A8), one can straightforwardly derive the $\mathbf{B}$'s in terms of the $\mathbf{U}$'s as given in (A9).

Although we do not show it in detail, we note that $\mathbf{B}$ is antisymmetric ($\mathbf{B}^{11^T} = -\mathbf{B}^{11}, \mathbf{B}^{21^T} = -\mathbf{B}^{12}$, etc.), which can be proved using

$$\begin{pmatrix}0 & 1\\ 1 & 0\end{pmatrix}\mathbf{M}\begin{pmatrix}0 & 1\\ 1 & 0\end{pmatrix} = -\mathbf{M}^T \quad \text{(A19)}$$

and

$$\begin{pmatrix}0 & 1\\ 1 & 0\end{pmatrix}\mathbf{U}\begin{pmatrix}0 & 1\\ 1 & 0\end{pmatrix} = (\mathbf{U}^{-1})^T. \quad \text{(A20)}$$

Now we must show the normalization C is of the form (A10). To do so, we find a differential equation for C. Letting

$$\hat{U}_{n+1} = \exp(-\Delta\beta\hat{h}_{n+1})\hat{U}_n, \quad \text{(A21)}$$

we define

$$\hat{U}_n(t) = \exp(-t\hat{h}_{n+1})\hat{U}_n, \quad \text{(A22)}$$

and so $\hat{U}_{n+1} = \hat{U}_n(\Delta\beta)$. Taking the expectation value of (A22) between FCS's, invoking (A11), and equating the parts independent of ξ, ξ^*, one obtains

$$\frac{d}{dt}\ln C_n(t) = -\text{Tr}\left[\Lambda(n+1)\mathbf{B}^{22}{}_n(t)\right]. \quad \text{(A23)}$$

Upon differentiating (A10), one obtains

$$\frac{d}{dt}\ln C_n(t) = \frac{1}{2}\text{Tr}\frac{d}{dt}\ln\mathbf{U}_n^{22}(t) - \frac{1}{2}\text{Tr}\Theta_{n+1}. \quad \text{(A24)}$$

Using $\mathbf{U}_n(t) = \exp(-\mathbf{M}_{n+1}t)\mathbf{U}_n$, one derives

$$\frac{d}{dt}\mathbf{U}_n^{22} = -2\Lambda_{n+1}\mathbf{U}^{12}{}_n + \Theta_{n+1}^T\mathbf{U}^{22} \quad \text{(A25)}$$

and (A24) becomes (A23). Thus Eq. (A10) satisfies the differential equation for C, and it just remains to establish the overall normalization. This is found by choosing

$\mathbf{M} = 0$, so that $\hat{U} = 1, C = 1$, and

$$\langle \xi | \hat{U} | \xi \rangle = \exp\left(-\sum_\alpha \xi_\alpha^* \xi_\alpha \right) , \quad\quad \text{(A26)}$$

which is $\langle \xi | \xi \rangle$. Thus we have established the form (A8) for $\langle \xi | \hat{U} | \xi \rangle$.

The integral (A5) is straightforward (see Berezin [13]); the magnitude is

$$\hat{\text{Tr}}\hat{U} = C \det \begin{pmatrix} \mathbf{B}^{11} & \mathbf{B}^{12} - \mathbf{1} \\ \mathbf{B}^{21} + \mathbf{1} & \mathbf{B}^{22} \end{pmatrix}^{\frac{1}{2}} . \quad\quad \text{(A27)}$$

The phase of $\hat{\text{Tr}}\hat{U}$, though critical, is more difficult to obtain (see Appendix B for details).

One can rewrite (A27) in a more compact form. The constant C contains the factor $\det(\mathbf{S}^{22})^{\frac{1}{2}}$, which can be

written using

$$\det \mathbf{U}^{22} = \det \begin{pmatrix} \mathbf{U}^{22} & \mathbf{U}^{12} \\ \mathbf{0} & \mathbf{1} \end{pmatrix}$$

$$= \det \begin{pmatrix} \mathbf{U}^{12^T} & \mathbf{U}^{22^T} \\ \mathbf{1} & \mathbf{0} \end{pmatrix} (-1)^{N_s^{\,2}} . \quad \text{(A28)}$$

Upon introducing (A28) into (A27), performing some algebra, and using relationships from (A20), one arrives at

$$\hat{\text{Tr}}\hat{U} = \det(\mathbf{1} + \mathbf{U})^{\frac{1}{2}} \exp\left(-\frac{\Delta\beta}{2} \text{Tr} \sum_{n=1}^{N_t} \Theta(n) \right) , \quad \text{(A29)}$$

where, again, $\mathbf{U}$ is the matrix in (A6) representing the evolution operator $\hat{U}$.

As for the density case, one can introduce an activity expansion to project out an exact particle number,

$$\hat{\text{Tr}}(\lambda^{\hat{N}}\hat{U}) = \det \left[\mathbf{1} + \begin{pmatrix} \boldsymbol{\lambda} & \mathbf{0} \\ \mathbf{0} & \frac{1}{\lambda} \end{pmatrix} \mathbf{U} \right]^{\frac{1}{2}} \exp\left(-\frac{\Delta\beta}{2} \sum_{n=1}^{N_t} \text{Tr}\Theta(n) \right) \lambda^{N_s/2} . \quad\quad\quad \text{(A30)}$$

Because the matrices $\mathbf{1}$ and $\mathbf{U}$ are of dimension $2N_s \times 2N_s$, one can write $\lambda^{N_s/2} = \det \begin{pmatrix} \mathbf{1} & \mathbf{0} \\ \mathbf{0} & \lambda^{\frac{1}{2}} \end{pmatrix}$ and (A30) becomes

$$\hat{\text{Tr}}\left(\lambda^{\hat{N}}\hat{U} \right) = \det \left[\begin{pmatrix} \mathbf{1} & \mathbf{0} \\ \mathbf{0} & \boldsymbol{\lambda} \end{pmatrix} + \begin{pmatrix} \boldsymbol{\lambda} & \mathbf{0} \\ \mathbf{0} & \mathbf{1} \end{pmatrix} \mathbf{U} \right]^{\frac{1}{2}} \times \exp\left(-\frac{\Delta\beta}{2} \sum_{n=1}^{N_t} \text{Tr}\Theta(n) \right) . \quad\quad\quad \text{(A31)}$$

This can be expanded into a polynomial in λ, which then gives the canonical ensemble.

Finally, we give the expectation value of $\langle \psi_t | \hat{U} | \psi_t \rangle$. First we note that the vacuum expectation value $\langle 0 | \hat{U} | 0 \rangle$ is the term in (A31) independent of λ,

$$\langle 0 | \hat{U} | 0 \rangle = \det \begin{pmatrix} \mathbf{1} & \mathbf{0} \\ \mathbf{0} & \mathbf{U}^{22} \end{pmatrix}^{1/2} \exp\left(-\frac{\Delta\beta}{2} \sum_n \text{Tr}\Theta(n) \right) \quad\quad\quad \text{(A32a)}$$

$$= \det \left[\begin{pmatrix} \mathbf{0} & \mathbf{1} \end{pmatrix} \mathbf{U} \begin{pmatrix} \mathbf{0} \\ \mathbf{1} \end{pmatrix} \right]^{\frac{1}{2}} \exp\left(-\frac{\Delta\beta}{2} \sum_n \text{Tr}\Theta(n) \right) . \quad\quad\quad \text{(A32b)}$$

Any quasiparticle excitations can be represented as Hartree-Fock-Bogoliubov vacua for properly defined new quasiparticle operators, which corresponds to doing a similarity transformation on the matrices. If $|\psi_t\rangle$ is the vacuum to the quasiparticle annihilation operator β_i; i.e.,

$$\beta_i | \psi_t \rangle = 0, \quad \beta_i = \mathbf{u}_{ij} a_j + \mathbf{v}_{ij} a_j^\dagger, \quad\quad\quad\quad\quad \text{(A33)}$$

then

$$\langle \psi_t | \hat{U} | \psi_t \rangle = \det \left[\begin{pmatrix} \mathbf{0} & \mathbf{1} \end{pmatrix} \begin{pmatrix} \mathbf{u} & \mathbf{v} \\ \mathbf{v}^* & \mathbf{u}^* \end{pmatrix} \mathbf{U} \begin{pmatrix} \mathbf{u}^\dagger & \mathbf{v}^T \\ \mathbf{v}^\dagger & \mathbf{u}^T \end{pmatrix} \begin{pmatrix} \mathbf{0} \\ \mathbf{1} \end{pmatrix} \right] \exp\left(-\frac{\Delta\beta}{2} \sum_n \text{Tr}\Theta(n) \right)$$

$$= \det \left[\begin{pmatrix} \mathbf{v}^* & \mathbf{u}^* \end{pmatrix} \mathbf{U} \begin{pmatrix} \mathbf{v}^T \\ \mathbf{u}^T \end{pmatrix} \right]^{\frac{1}{2}} \exp\left(-\frac{\Delta\beta}{2} \sum_n \text{Tr}\Theta(n) \right) . \quad\quad\quad\quad\quad \text{(A34)}$$

APPENDIX B: SIGN OF THE OVERLAP FOR PAIRING FIELDS

The formulas derived in Appendix A for calculating the overlap $\zeta_\sigma(\beta) = \langle \psi_L | \hat{U}(\beta, 0; \sigma) | \psi_R \rangle$ in the zero-temperature formalism and $\hat{\mathrm{Tr}}[\hat{U}_\sigma(\beta, 0)]$ in the thermal formalisms all involve the square root of a determinant, leaving the phase of $\zeta_\sigma(\beta)$ undetermined by a factor of ± 1. This ambiguity is irrelevant for the Monte Carlo random walk as we typically take $|\zeta|$ as the weight function, but the phase must be known unambiguously for calculation of observables, as important cancellations may result.

We determine the phase by following the evolution of $\zeta_\sigma(\tau)$ and its derivatives with respect to τ as τ goes from 0 to β. For example, if $\zeta_\sigma(\tau)$ were purely real, zero crossing [with $\zeta'(\tau) \neq 0$] would indicate a change in the phase by -1. The initial phase at $\tau = 0$ is real and positive. Following the evolution is computationally expensive, but as most of the time is spent on the random walk, where the phase is irrelevant, the overall computational time is negligible.

In what follows we give the formulae for up to fourth derivatives for each of the different formalisms.

1. Grand-canonical ensemble

Define

$$f(t) = \zeta_\sigma(k\Delta\beta + t) = \hat{\mathrm{Tr}}[e^{-h_{k+1}t} \hat{U}_\sigma(k\Delta\beta, 0)]; \quad \text{(B1)}$$

then

$$f(t) = \det[1 + e^{-\mathbf{M}_{k+1}t}\mathbf{U}]^{\frac{1}{2}} \times \exp\left(-\frac{\Delta\beta}{2}\sum_{i=1}^{k}\mathrm{Tr}[\Theta_i] - \frac{t}{2}\mathrm{Tr}[\Theta_{k+1}]\right), \quad \text{(B2)}$$

$$\ln(f) = \frac{1}{2}\mathrm{Tr}[\ln(1 + e^{-\mathbf{M}_{k+1}t}\mathbf{U})] - \frac{\Delta\beta}{2}\sum_{i=1}^{k}\mathrm{Tr}[\Theta_i] - \frac{t}{2}\mathrm{Tr}[\Theta_{k+1}]. \quad \text{(B3)}$$

Using the abbreviation $\mathbf{M} = \mathbf{M}_{k+1}, \Theta = \Theta_{k+1}$, let

$$\mathbf{G} = (1 + e^{-\mathbf{M}t}\mathbf{U})^{-1}e^{-\mathbf{M}t}\mathbf{U} = 1 - (1 + e^{-\mathbf{M}t}\mathbf{U})^{-1}, \quad \text{(B4)}$$

$$\frac{\partial \mathbf{G}}{\partial t} = -[1 + e^{-\mathbf{M}t}\mathbf{U}]^{-1}\mathbf{M}e^{-\mathbf{M}t}\mathbf{U}[1 + e^{-\mathbf{M}t}\mathbf{U}]^{-1}$$
$$= -(1 - \mathbf{G})\mathbf{M}\mathbf{G}. \quad \text{(B5)}$$

The derivatives of $\ln(f)$ can be expressed in terms of the matrices $\mathbf{G}$ and $\mathbf{M}$,

$$g_1 \equiv \frac{\partial \ln(f)}{\partial t} = -\frac{1}{2}\mathrm{Tr}[\mathbf{M}\mathbf{G}] - \frac{1}{2}\mathrm{Tr}[\Theta], \quad \text{(B6)}$$

$$g_2 \equiv \frac{\partial^2 \ln(f)}{\partial t^2} = \frac{1}{2}\mathrm{Tr}[\mathbf{M}(1 - \mathbf{G})\mathbf{M}\mathbf{G}], \quad \text{(B7)}$$

$$g_3 \equiv \frac{\partial^3 \ln(f)}{\partial t^3} = -\frac{1}{2}\mathrm{Tr}[\mathbf{M}\mathbf{G}\mathbf{M}(1 - \mathbf{G})\mathbf{M}(1 - 2\mathbf{G})], \quad \text{(B8)}$$

$$g_4 \equiv \frac{\partial^4 \ln(f)}{\partial t^4} = -\frac{1}{2}\mathrm{Tr}[\mathbf{M}(1 - \mathbf{G})\mathbf{M}\mathbf{G}\mathbf{M}(1 - \mathbf{G})\mathbf{M}(1 - 2\mathbf{G})]$$
$$-\frac{1}{2}\mathrm{Tr}[\mathbf{M}\mathbf{G}\mathbf{M}(1 - \mathbf{G})\mathbf{M}\mathbf{G}\mathbf{M}(1 - 2\mathbf{G})] - \mathrm{Tr}[\mathbf{G}\mathbf{M}(1 - \mathbf{G})\mathbf{M}(1 - \mathbf{G})\mathbf{M}\mathbf{G}\mathbf{M}]. \quad \text{(B9)}$$

Then $\zeta_\sigma(k\Delta\beta + t)$ is given by

$$\zeta_\sigma(k\Delta\beta + t) = f(t) = f(0)\exp\left(g_1 t + g_2\frac{t^2}{2!} + g_3\frac{t^3}{3!} + g_4\frac{t^4}{4!} + \cdots\right). \quad \text{(B10)}$$

2. Zero-temperature formalism

In this case

$$f(t) = \zeta_\sigma(k\Delta\beta + t) = \langle \psi_t | e^{-\hat{h}_{k+1}t}\hat{U}(k\Delta\beta, 0; \sigma)|\psi_t\rangle = \langle \psi_{\mathrm{L}}|e^{-\hat{h}_{k+1}t}|\psi_R\rangle, \quad \text{(B11)}$$

$$= \det[\boldsymbol{\Psi}_L e^{-\mathbf{M}_{k+1}t}\boldsymbol{\Psi}_R]^{\frac{1}{2}}e^{-\frac{\Delta\beta}{2}\sum_{i=1}^{k}(\mathrm{Tr}[\Theta_i] - \frac{t}{2}\mathrm{Tr}[\Theta_{k+1}])}, \quad \text{(B12)}$$

$$\ln(f) = \frac{1}{2}\text{Tr}[\ln(\boldsymbol{\Psi}_L e^{-\mathbf{M}_{k+1}t}\boldsymbol{\Psi}_R)] - \frac{\Delta\beta}{2}\sum_{i=1}^{k}\text{Tr}[\Theta_i] - \frac{t}{2}\text{Tr}[\Theta_{k+1}]. \tag{B13}$$

Let

$$\mathbf{G} = e^{-\mathbf{M}t}\boldsymbol{\Psi}_R[\boldsymbol{\Psi}_L e^{-\mathbf{M}t}\boldsymbol{\Psi}_R]^{-1}\boldsymbol{\Psi}_L \tag{B14}$$

$$\frac{\partial \mathbf{G}}{\partial t} = e^{-\mathbf{M}t}\boldsymbol{\Psi}_R[\boldsymbol{\Psi}_L e^{-\mathbf{M}t}\boldsymbol{\Psi}_R]^{-1}\boldsymbol{\Psi}_L \mathbf{M}e^{-\mathbf{M}t}\boldsymbol{\Psi}_R[\boldsymbol{\Psi}_L e^{-\mathbf{M}t}\boldsymbol{\Psi}_R]^{-1}\boldsymbol{\Psi}_L - \mathbf{M}e^{-\mathbf{M}t}\boldsymbol{\Psi}_R[\boldsymbol{\Psi}_L e^{-\mathbf{M}t}\boldsymbol{\Psi}_R]^{-1}\boldsymbol{\Psi}_L$$
$$= \mathbf{GMG} - \mathbf{MG} = -(\mathbf{1} - \mathbf{G})\mathbf{MG}. \tag{B15}$$

Then

$$g_1 = \frac{\partial \ln(f)}{\partial t} = -\frac{1}{2}\text{Tr}[\mathbf{MG}] - \frac{1}{2}\text{Tr}[\Theta], \tag{B16}$$

and so on and all formulas are the same as in the grand-canonical ensemble (B6–9), except that the matrix $\mathbf{G}$ is now different. In fact, in both cases $\mathbf{G}$ can be shown to be the matrix for the Green's function, i.e.,

$$\mathbf{G}_{ij} = \langle \alpha_j^\dagger \alpha_i \rangle, \tag{B17}$$

where

$$\alpha_i = a_i, i = 1, \ldots, N_s, \tag{B18a}$$

$$\alpha_{i+N_s} = a_i^\dagger, i = 1, \ldots, N_s. \tag{B18b}$$

3. Canonical ensemble

In Eq. (4.35), the undetermined sign involves only the vacuum expectation $\langle 0|\hat{U}(\beta,0)|0\rangle$. Once it is determined, the sign for $\hat{\text{Tr}}[\hat{U}(\beta,0)]$ is known. We can use the equations for the zero-temperature formalism to obtain the sign of $\langle 0|\hat{U}(\beta,0)|0\rangle$.

APPENDIX C: MAXIMUM ENTROPY EXTRACTION OF THE STRENGTH FUNCTION

We use the maximum entropy (ME) method to reconstruct the strength function from the response function. Here we give a brief description of the classic ME method; details can be found in the paper by Gull [19].

The ME method is a Bayesian approach for reconstruction of positive additive images f from noisy data. In our case the image is the strength function $f(\omega)$. The noisy data, $D_j = d_j + \eta_j$, are the measurements of the response function $R(\tau)$ at the discrete imaginary times, where $d_j = R(j\Delta\beta)$ and η_j is the noise in the data. In the absence of any data, the most probable image is chosen to be a default model m. Skilling [18] proved that, in that case, the only consistent choice for the probability of an image f is determined up to a parameter α:

$$pr(f) = \exp[\alpha S(f,m)]/Z(\alpha,m), \tag{C1}$$

where S is the entropy of image f relative to the default model. If the image is discretized to f_i ($i = 1, \ldots, r$), then

$$S(f,m) = \sum_j[f_j - m_j - f_j\ln(f_j/m_j)] \tag{C2}$$

and

$$Z_S(\alpha,m) = \int_0^\infty d^r f \prod f^{-\frac{1}{2}}\exp[\alpha S(f)]$$
$$= \int_{-\infty}^\infty d^r u \exp[\alpha S(u^2)], \tag{C3}$$

where the last step follows from a change of variable $u_i = \sqrt{f_i}$. (Z_S has no relation to the nuclear partition function.)

In the presence of data, we gain some knowledge about the image. Assuming a Gaussian distribution of errors in the data D_i, the probability for f is

$$pr(f) = \exp[\alpha S - \tfrac{1}{2}\chi^2(f)]\frac{1}{Z_S}\frac{1}{Z_L}, \tag{C4}$$

where

$$\chi^2(f) = \sum[d_i(f) - D_i)(d_j(f) - D_j]G_{ij}^{-1}, \tag{C5}$$

$G_{ij} = \langle \eta_i \eta_j \rangle$ is the correlation matrix of the errors in the data, and

$$Z_L = \int d^N D \exp[-\tfrac{1}{2}\chi^2(f)]. \tag{C6}$$

For a given choice of α, the most probable image can be found by maximizing $\alpha S - \frac{1}{2}\chi^2$, giving rise to the term "maximum entropy" method. However, α is not predetermined. Rather, it is varied until χ^2 at the maximum of $\alpha S - \frac{1}{2}\chi^2$ is approximately equal to the total number of data D_i. But this assignment of α is ad hoc and, according to Gull [19], usually leads to an underfitting of the data. In the classic ME, α is fixed by maximizing the probability of α given the data set D_i and the default model m:

$$pr(\alpha|D,m) \propto Z_Q Z_S^{-1} Z_L^{-1}, \tag{C7}$$

where

$$Z_Q = \int_0^\infty d^r f \prod f^{\frac{1}{2}} \exp(\alpha S - \tfrac{1}{2}\chi^2)$$

$$= \int_{-\infty}^\infty d^r u \, \exp(\alpha S - \tfrac{1}{2}\chi^2) \,. \qquad \text{(C8)}$$

After α is fixed, we can find the most probable f by maximizing $\alpha S - \frac{1}{2}\chi^2$, or we can find the average f by Monte Carlo sampling using the integrand of (C4) as weight function. Information about the uncertainty in f can also be obtained from Monte Carlo sampling. In the particular application at hand, we would like to know, for example, the uncertainty in the location of the peaks in f, or in the moments $M_n = \int \tilde{f}(\omega)\omega^n d\omega / \int \tilde{f}(\omega) d\omega$.

Let us now return to the problem of extracting the strength function. Since the imaginary-time response function $R(\tau)$ is given at discrete times, we can only allow a limited amount of parameters in the strength function $\tilde{f}$, which we do by discretizing $\tilde{f}(\omega)$ to f_i at ω_i. To allow for some smoothness, we choose a Gaussian function centered around each ω_i, rather than a delta function. Given the imaginary-time response function, we bound the range of ω over which the f is significant by $\omega_{\min}$ and $\omega_{\max}$, and choose the ω_i to be evenly distributed between them. The number of f_n, n_ω, should not exceed the number of data D_i we have, which is the total number of time slices, Nt. We choose the width of each Gaussian, $\Delta\omega$, to be half of the spacing between the ω_i's. For a non-Hermitian operator $\hat{O}$, the strength function $f(\omega)$ is related to f_i by

$$f(\omega) = \sum_i f_i \exp[-\tfrac{1}{2}(\omega - \omega_i)^2/\Delta^2\omega]\frac{1}{\Delta\omega\sqrt{2\pi}} \,, \qquad \text{(C9)}$$

while for a Hermitian operator, $f(-\omega) = e^{-\beta\omega}f(\omega)$ in the canonical ensemble, and we choose

$$f(\omega) = \sum_i f_i e^{\beta/2(\omega-\omega_i)}[e^{-1/2(\omega-\omega_i)^2/\Delta\omega^2}$$
$$+ e^{-1/2(\omega+\omega_i)^2/\Delta\omega^2}]\frac{1}{\Delta\omega\sqrt{2\pi}} \,. \qquad \text{(C10)}$$

The response $R(\tau)$ generated by $f(\omega)$ is, for non-Hermitian operators,

$$R(\tau) = \sum_i f_i e^{(-\omega_i\tau + \frac{1}{2}\tau^2\Delta\omega^2)} \,, \qquad \text{(C11)}$$

while for Hermitian operators it is

$$R(\tau) = \sum_i f_i(e^{(-\tau\omega_i)} + e^{-(\beta-\tau)\omega_i}e^{\frac{1}{2}(\frac{\beta}{2}-\tau)^2\Delta\omega^2}) \,. \qquad \text{(C12)}$$

We choose the default model m_i, $i = 1,\ldots,n_\omega$, to be a constant fixed by $R(0)$, which is related to the total strength. The data D_j are the values of $R(\tau)$ for $\tau = j\Delta\beta$ measured from the Monte Carlo sampling. The error correlation function can also be measured in these calculations.

To maximize the probability (C7), we have to know the dependence of Z_S and Z_Q on α. Some simplification can be had by calculating Z_S in the saddle point approximation. There is a saddle point in $S(u^2, m)$ at $u_i^2 = m_i$ with the second derivatives $\frac{\partial S}{\partial u_i \partial u_j}|_{u_i^2 = m_i} = -4\delta_{ij}$, which leads to the approximate integral

$$\int_{-\infty}^\infty d^r u \, \exp(\alpha S) \simeq \int_{-\infty}^\infty d^r u \, \exp\left(-2\alpha \sum_i u_i^2\right)$$
$$= \left(\frac{\pi}{2\alpha}\right)^{r/2} \,. \qquad \text{(C13)}$$

The condition $\frac{\partial p}{\partial \alpha} = 0$ then becomes

$$\frac{1}{Z_Q}\int_{-\infty}^\infty d^r u \, S \exp(\alpha S - \tfrac{1}{2}\chi^2) = \frac{1}{Z_S}\frac{\partial Z_S}{\partial \alpha} = -\frac{r}{2\alpha} \qquad \text{(C14)}$$

and the average image $\langle f_i \rangle$ is given by

$$\langle f_i \rangle = \frac{1}{Z_Q}\int_{-\infty}^\infty d^r u \, f_i \exp(\alpha S - \tfrac{1}{2}\chi^2) \,. \qquad \text{(C15)}$$

We do these integrals by Monte Carlo sampling of u_i with $\exp(\alpha S - \frac{1}{2}\chi^2)$ as the weight function. The value α is determined by the self-consistent condition $\langle S \rangle_\alpha = -\frac{r}{2\alpha}$. When α is known, the average distribution $\langle f_i \rangle = \langle u_i^2 \rangle$ and the uncertainty $\delta f_i = \sqrt{\langle f_i^2 \rangle - \langle f_i \rangle^2}$ is also given in the course of the Monte Carlo evaluation of (C15).

[1] B. H. Wildenthal, Prog. Part. Nucl. Phys. **11**, 5 (1984).

[2] B. H. Wildenthal, in *Shell Model and Nuclear Structure: Where Do We Stand?*, 2nd International Spring Seminar on Nuclear Physics, edited by A. Covello (World Scientific, Singapore, 1988).

[3] W. von der Linden, Phys. Rep. **220**, 53 (1992), and references therein.

[4] S. E. Koonin, G. Sugiyama, and H. Friederich, in *Proceedings of the Conference on TDHF and Beyond*, Lecture Notes in Physics, Vol. 171, edited by K. Goeke (Springer, Heidelberg, 1982); G. Sugiyama and S. E. Koonin, Ann. Phys. (N.Y.) **168**, 1 (1986).

[5] J. Hubbard, Phys. Lett. **3**, 77 (1959); R. D. Stratonovich, Dokl. Akad. Nauk. SSSR **115**, 1907 (1957) [Sov. Phys.

Dokl. **2**, 416 (1958)].

[6] J. E. Hirsch, Phys. Rev. B **28**, 4059 (1983).

[7] C. W. Johnson, S. E. Koonin, G. H. Lang, and W. E. Ormand, Phys. Rev. Lett. **69**, 3157 (1992).

[8] P. Arve, G. Bertsch, B. Lauritzen, and G. Puddu, Ann. Phys. (N.Y.) **183**, 309 (1988); B. Lauritzen and G. Bertsch, Phys. Rev. C **39**, 2412 (1989); B. Lauritzen, P. Arve, and G. F. Bertsch, Phys. Rev. Lett. **61**, 2835 (1988); Y. Alhassid and B. W. Bush, Nucl. Phys. **A549**, 43 (1992).

[9] G. Puddu, P. F. Bortignon, and R. A. Broglia, Ann. Phys. (N.Y.) **206**, 409 (1991); Phys. Rev. C **42**, R1830 (1990).

[10] D. J. Thouless, *The Quantum Mechanics of Many Body*

Systems (Academic Press, New York, 1961).

[11] B. A. Brown, A. Etchegoyen, and W. D. M. Rae, MSU-NSCL Report No. 524, 1985.

[12] W. E. Ormand, D. J. Dean, C. W. Johnson, G. H. Lang, and S. E. Koonin, submitted to Phys. Rev. C.

[13] F. A. Berezin, *The Method of Second Quantization* (Academic Press, New York, 1966).

[14] E. Y. Loh, Jr. and J. E. Gubernatis, in *Electronic Phase Transitions*, edited by W. Hanke and Yu. V. Kopaev (Elsevier Science Publishers B.V., New York, 1992).

[15] J. Dobaczewski and S. E. Koonin, Caltech Report No. MAP-35, 1983 (unpublished).

[16] S. R. White, D. J. Scalapino, R. L. Sugar, and N. E. Bickers, Phys. Rev. Lett. **63**, 14 (1989); S. R. White,

Phys. Rev. B **46**, 5678 (1992).

[17] R. N. Silver, J. E. Gubernatis, D. S. Sivia, and M. Jarell, Phys. Rev. Lett. **65**, 496 (1990); R. N. Silver, D. S. Sivia, and J. E. Gubernatis, Phys. Rev. B **41**, 2380 (1990).

[18] J. Skilling, in *Maximum Entropy and Bayesian Methods*, edited by J. Skilling (Kluwer Academic, Boston, 1989), p. 45.

[19] S. F. Gull, in [18], p. 53.

[20] E. Y. Loh, Jr., J. E. Gubernatis, R. T. Scalettar, S. R. White, D. J. Scalapino, and R. L. Sugar, Phys. Rev. B **41**, 9301 (1990); S. B. Fahy and D. R. Hamann, *ibid.* **43**, 765 (1991).

[21] J. W. Negele and H. Orland, *Quantum Many-Particle Systems* (Addison-Wesley, Redwood City, 1988).